CONFIDENTIAL

285

Copy
RM E52I10

NACA RM E52I10

6773

NACA

RESEARCH MEMORANDUM

EFFECT OF ROTOR- AND STATOR-BLADE MODIFICATIONS ON SURGE

PERFORMANCE OF AN 11-STAGE AXIAL-FLOW COMPRESSOR

II - REDESIGNED COMPRESSOR FOR XJ40-WE-6 ENGINE

By E. William Conrad, Harold B. Finger, and Robert H. Essig

Lewis Flight Propulsion Laboratory
Cleveland, Ohio

Classification cancelled (or changed to ...Unclassified...........)

By ...... NASA Tech Pub Announcement th
        (OFFICER AUTHORIZED TO CHANGE)

By ....   18 Dec 58

GRADE OF OFFICER MAKING CHANGE)

31 Mar 64
DATE

NATIONAL ADVISORY COMMITTEE
FOR AERONAUTICS
WASHINGTON
May 25, 1953

CONFIDENTIAL

2702

NATIONAL ADVISORY COMMITTEE FOR AERONAUTICS

RESEARCH MEMORANDUM

EFFECT OF ROTOR- AND STATOR-BLADE MODIFICATIONS ON SURGE PERFORMANCE

OF AN 11-STAGE AXIAL-FLOW COMPRESSOR

II - REDESIGNED COMPRESSOR FOR XJ40-WE-6 ENGINE

By E. William Conrad, Harold B. Finger, and Robert H. Essig

SUMMARY

An investigation to increase the compressor surge-limit pressure
ratio of the XJ40-WE-6 turbojet engine at high equivalent speeds was
conducted at the NACA Lewis altitude wind tunnel. Evaluated herein
are a basic redesign of the compressor and 11 additional modifications
which included twisting rotor blades (in place) to change blade section
angles, inserting new stator diaphragms with different blade section
angles, and opening the inlet guide vanes. By means of a variable-area
first-stage turbine-nozzle diaphragm, the surge-limit pressure ratio
of each configuration was determined over a range of equivalent engine
speeds from about 4800 to 8000 rpm at an altitude of 30,000 feet and a
flight Mach number of 0.64. The surge limit for several configurations
was also obtained at altitudes of 15,000 and 45,000 feet at a flight
Mach number of 0.21. Complete performance maps of the final compressor
configuration were obtained for a flight Mach number of 0.64 at
altitudes of 15,000, 35,000 and 45,000 feet and for a flight Mach
number of 1.00 at an altitude of 35,000 feet.

It was found that a compressor redesigned to satisfy more closely
simple radial equilibrium requirements at the inlet and exit stages
and the additional modifications of the final configuration resulted
in an appreciable improvement in the compressor surge limit over that
of the original production compressor at high equivalent engine speeds.
Opening the inlet guide vanes 5° increased the engine air flow, and
thus the thrust, approximately 5 percent above that of the basic
redesigned compressor.

INTRODUCTION

Preliminary performance tests of the XJ40-WE-6 turbojet engine
in the NACA Lewis altitude wind tunnel revealed a severe surge condition

in the compressor at high equivalent engine speeds. Avoidance of compressor surge required a thrust reduction of approximately 20 percent below the expected value. Almost simultaneously the same difficulty was reported by an airframe manufacturer using this engine in a prototype airplane.

A program to increase the surge-limit pressure ratio of the XJ40-WE-6 engine was immediately initiated. In view of the fact that production had been started and a small number of engines were already in the field, the surge program was divided into two distinct phases: (a) to remove the thrust limitation resulting from compressor surge on existing engines by compressor modifications that could be quickly and conveniently incorporated on engines in the field and (b) to provide, for future production engines, a compressor configuration combining good efficiency and air-flow characteristics with a greater surge margin. The results of phase (a) are presented in reference 1 and those of phase (b) are contained in this report.

The design analysis and interstage performance data of the original compressor (reference 1) indicated that simple radial equilibrium requirements were not satisfied in the inlet and exit stages. A basic redesign to satisfy these requirements called for changes in the rotor-blade section angles. Similar conclusions had been reached independently by the engine manufacturer prior to the altitude operation of the original compressor, and an engine which included reslotted rotor disks was partially completed. This engine was subsequently used as the basic test vehicle in this investigation.

Several modifications were made to the redesigned compressor in order to investigate the effects on over-all performance of the various blade-angle adjustments considered to be beneficial for eliminating the high-speed surge problem, to improve the flow distribution leaving the compressor, to take into account simple radial equilibrium requirements at inlet and exit stages, and to investigate the effect of discharge-flow resistance on the compressor surge limit. The methods which were considered for modifying various configurations of the redesigned compressor are as follows:

(1) Twisting rotor blades (in place) to change blade section angles

(2) Inserting new stator diaphragms with different blade angles

(3) Modifying the second blade row of the outlet guide-vane assembly

(4) Opening the inlet guide vanes

2702

Each configuration resulting from one or more of the above modifications was successively evaluated, and its effect on performance characteristics was used to guide the next modification. The relative merit of each configuration was determined by its surge limit and air-flow characteristics over a range of equivalent engine speeds. A variable-area turbine-nozzle diaphragm, supplied by the engine manufacturer, permitted steady-state engine operation up to the surge limit without exceeding turbine temperature limitations.

APPARATUS AND PROCEDURE

Description of Engine

The engine discussed hereinafter was designated as an XJ40-WE-6 engine but differed appreciably from the initial production version. When the engine was received from the manufacturer, the rotor of the redesigned compressor differed from that of the original production compressor as follows:

(a) First rotor closed (unloaded) at tip and opened (loaded) at hub

(b) Second rotor closed at tip

(c) Rotors 5 to 9 closed by reslotting rotor disks

(d) Eleventh rotor opened at hub and closed at tip

The design static sea-level performance of the production model was 7500 pounds thrust at an equivalent engine speed of 7260 rpm and a turbine-inlet gas temperature of 1885° R. Compressor pressure ratio was 5:1 at an air weight flow of 140 pounds per second. Main components of the engine (fig. 1) included an 11-stage axial-flow compressor, a single-annular combustor, a two-stage turbine, an exhaust collector, and a continuously variable clam-shell-type exhaust nozzle. Primary control of the engine was accomplished electronically, and emergency protection was provided by a hydraulic control. Over-all length of the engine was 186 inches and the dry weight was 2981 pounds. Height and width of the engine including accessories were 45.5 and 42.4 inches, respectively.

Air ducting to the compressor consisted of two elliptical engine inlets, one on either side of the accessory gear case, as shown in figure 2. The air passages join to form an annulus approximately 2 inches ahead of the inlet guide vanes. A view of the compressor with the top half of the casing removed is shown in figure 3. The

11-stage rotor was followed by two rows of outlet guide vanes to provide axial flow into the combustor. During part of this investigation, a "mixer" section, supplied by the engine manufacturer, was substituted for the second row of outlet guide vanes. The mixer consisted essentially of twisted guide vanes in which adjacent blades were twisted in opposite directions. The purpose of the mixer was to intermix the high-energy air at the rotor tip with the low-energy air at the root in an effort to control radial temperature distribution at the turbine inlet. In addition to the standard outlet guide-vane assembly and the mixer section, a modified outlet guide-vane assembly was also used in an effort to improve the surge limit. The modified assembly consisted of a standard assembly in which alternate blades of the second blade row were removed to decrease the solidity.

A variable-area first-stage turbine-nozzle diaphragm (fig. 4) was also supplied by the engine manufacturer. As will be discussed in the section Procedure, this proved to be an excellent research tool in evaluating the surge limits of the various configurations quickly and accurately.

Installation

As shown in figure 1, the engine was mounted on a wing spanning the test section of the altitude wind tunnel. Dry refrigerated air was supplied to the engine from the tunnel make-up air systems through a duct connected to the engine inlet. Manually controlled butterfly valves in this duct were used to adjust air total pressures at the engine inlet. A slip joint with a frictionless seal was used in the duct, thereby making possible the measurement of thrust and drag with the tunnel scales.

Instrumentation for measuring pressures and temperatures was installed at various stations in the engine (fig. 5) to determine the steady-state performance. A schematic diagram showing the location of the instrumentation in the compressor is given in figure 6. A traverse mechanism comprising 10 sonic-type thermocouples (reference 2) was supplied by the engine manufacturer to determine the gas temperature pattern at the turbine inlet.

Procedure

Symbols and a method of calculation are given in appendices A and B, respectively. The air flow through the make-up air duct was throttled from approximately sea-level pressure to a total pressure at the engine inlet corresponding to the desired flight Mach number

2702

at a given altitude. The static pressure in the tunnel test section was
maintained to correspond to the desired altitude. Engine-inlet-air
temperatures were held at approximately NACA standard values corres-
ponding to the simulated flight conditions, except for high altitudes
and low flight Mach numbers. No inlet-air temperatures below about
-20° F were obtained.

The original production engine configuration had surge character-
istics such that it was necessary to operate at turbine-inlet tempera-
tures below military rated (1885° R) at high equivalent engine speeds to
avoid compressor surge. Consequently, it was possible to determine the
compressor surge limits simply by closing the exhaust nozzle at constant
engine speed until surge occurred. For later configurations, where the
surge limit was above the limiting temperature operating line with the
standard turbine area, the variable-area turbine nozzle was used to
allow operation up to the surge limit without encountering limiting
turbine temperature. The data of figure 7 illustrate the large changes
in compressor pressure ratio which could be obtained at constant engine
temperature ratio by changing the turbine-nozzle area. Although not
shown, the variable-area turbine diaphragm could be closed much further
to provide high compressor pressure ratios at the low engine temperature
ratios.

Most of the data were obtained at equivalent engine speeds between
4800 and 8000 rpm at an altitude of 30,000 feet and a flight Mach
number of 0.64. In addition, surge data were obtained on several
configurations at altitudes of 15,000 and 45,000 feet at a flight
Mach number of 0.21 to determine the effect of varying flight condition.

For the final compressor configuration, steady-state performance
maps were obtained at a flight Mach number of 0.64 for altitudes of
15,000, 35,000, and 45,000 feet and at a flight Mach number of 1.00 for
an altitude of 35,000 feet. Five fixed positions of the variable-area
exhaust nozzle were used for each flight condition, and equivalent
engine speed was varied from 4800 to 8000 rpm.

COMPRESSOR REDESIGN AND MODIFICATIONS

Compressor Redesign

The compressor of the XJ40-WE-6 turbojet engine was an 11-stage
unit having a rotor tip diameter of 32.14 inches and an inlet hub-tip
ratio of 0.6. It was initially designed to handle a specific air
weight flow of 24.2 pounds per second per square foot at a pressure
ratio of 4.6:1 and a speed of 7260 rpm. Mismatching between the
compressor and turbine was encountered at the start of the development

program, and the compressor stator and rotor blades were reset by the
manufacturer so as to shift the design point for the original production
engine to a pressure ratio of 5:1 and the specific weight flow to
24.8 pounds per second per square foot.

The analysis of the design of the compressor, as given in refer-
ence 1, indicated that radial equilibrium requirements were not satisfied
in the inlet and exit stages. Neglect of radial equilibrium conditions
at the inlet resulted in the first rotor tip section stalling and the
hub section approaching a turbining condition at design speed. The
subject compressor is a redesign of the compressor discussed in refer-
ence 1 to satisfy more closely radial equilibrium requirements. The
blade-angle settings in the first rotor were changed so that the hub
section was opened approximately 3° and the tip section was closed
approximately 4°. This change loaded the hub section and unloaded the
mean and tip sections. The rotor of the second stage was twisted
closed at the tip approximately 4° so that this section was unloaded
while the hub-section angle remained unaltered. The stator changes
required to satisfy radial equilibrium requirements in the first
three stages of the compressor were not incorporated in the original
build-up of the compressor but were incorporated in the compressor
modifications. The rotors of the fifth to ninth stages were all
unloaded by resetting the blades in the root fastenings approximately
3° to 5°. (The investigation of reference 1 indicates that the hub
sections of the seventh and eighth stages were stalled.) The
eleventh-stage rotor was loaded by approximately 3° at the root section
and unloaded by about 3° at the tip section. All remaining blade
rows were identical with those of the standard configuration of refer-
ence 1. These changes completed the basic redesign of the compressor,
designated hereinafter as configuration A.

Compressor Modifications

As shown by the analysis of compressor off-design performance of
reference 3 and other experimental investigations, the operational
characteristics of axial-flow compressors are such that, at speeds
below design speed, the inlet stages of the compressor operate at
extremely high angles of attack and thus stall while the exit stages
operate at low angles of attack near the turbining region. At speeds
above design speed, however, the inlet stages operate near the
choking or turbining region, while the exit stages operate at high
angles of attack and approach a stalled condition. Thus, improve-
ment in the high-speed surge limit of an axial-flow compressor
requires that the exit stages of the unit be unstalled or that the
angle of attack be reduced on these stages. Reducing the angle of
attack can be accomplished to some extent by adjusting stator - or

2702

2702

rotor-blade section angles in the direction of unloading the rear end of the compressor. However, references 1 and 3 indicate that the effects of such changes are usually small. In addition to unloading the rear stages of the compressor, loading the inlet stages of the compressor by blade-angle adjustment might also increase the surge-limit pressure ratio at high speeds. It would be expected that such modifications would seriously hurt the low-speed surge characteristics of the compressor because the front end of the compressor would be operating at even higher angles of attack than originally and the exit stages would be even further into the turbining region. Actually, a change in compressor weight flow and a shift in axial-velocity distribution accompanies the changes in blade-angle setting so that conditions at speeds below design speed are not as seriously affected as might be expected.

Thus an attempt was made to increase the surge-limit pressure ratio of the redesigned compressor at high equivalent speeds by means of additional modifications to unload the rear half of the compressor. The various configurations resulting from these modifications are listed in table I. Configurations A and B were directed toward satisfying radial equilibrium requirements in the inlet stages. Configuration C was an attempt to satisfy more closely radial equilibrium requirements in the exit stages. In configurations D and E the hub and tip sections of the last two stages were unloaded by different amounts in an effort to determine whether the hub or tip sections of these stages were most critically loaded at high equivalent speeds. A reduced-solidity outlet guide vane was used in configurations F and G to determine the effect of low solidity, or decreased resistance, on the high-speed surge limit. The inlet guide vanes were opened 5° in configuration H in an effort to further load the first rotor hub and increase the air flow. Configuration I again unloaded the last two stages at high speeds and configuration J evaluated the effect of the mixer on the surge limit. Configuration K evaluated the relative merit of the modified and production stators in the first, second, and third stages. Configuration L was an attempt to improve the turbine-inlet temperature distribution by improving the flow distribution out of the compressor. The final configuration (M) resulted from configuration J in which the variable-area turbine-nozzle diaphragm was replaced with the fixed-area production-nozzle diaphragm.

RESULTS AND DISCUSSION

Performance of Basic Redesign

Design and experimental pressure-ratio distributions are presented in figure 8 for several stages of the redesigned compressor. The

excellent agreement obtained for the first stage indicates that the hub turbining conditions discussed in reference 1 have been reduced at design speed. At speeds above design, however, the hub is probably still turbining because of the reduced angle of attack on the first stage as speed is increased. Although the first-stage distributions agree very well, the measured pressure rise in later stages is noticeably greater than the design values. This difference in pressure ratio increases progressively through the compressor so that at the eleventh-stator inlet the actual average pressure ratio is 5.15:1 while the design pressure ratio is 4.65:1. The increased loading in the later stages is due partly to the increased loading in the first stage resulting from the resetting of the first rotor and partly to the resetting of the fifth to ninth stages. These resettings appear to have reduced the stalling problems in the seventh and eighth stages discussed in reference 1.

The surge limit of the redesigned compressor is presented in figure 9 on the basis of equivalent engine speed. Data obtained for flight Mach numbers of 0.64 and 0.21 at altitudes of 30,000 and 45,000 feet, respectively, indicate that altitude has little effect on the surge limit. For comparison, the surge limits of both the original production compressor and the best modification of the original compressor (reference 1) are also shown. Although a critical comparison of two different build-ups of the same model engine (configuration A and original compressor) is not entirely valid, figure 9 indicates that the redesigned compressor has a desirable surge limit.

Effect of Modifications on Performance

The effects of the various modifications on the surge limit and air flow of the XJ40-WE-6 redesigned compressor are summarized in the bar graphs of figures 10 and 11. For comparison, a bar for the best modification of the original compressor (reference 1) is also included. Surge pressure ratios are presented for equivalent engine speeds of 6000, 7260 (rated sea level), 7800, and 8000 rpm in figure 10, while the compressor-air weight flows are shown in figure 11 for equivalent engine speeds of 7260, 7800, and 8000 rpm. Air flows for configuration B are not presented because icing conditions on the instrumentation resulted in inaccurate measurements. Up to configuration H the effects of the modifications on the performance of the basic redesigned compressor are small.

A description of the various configurations resulting from one or more modifications and a discussion of the effect of each modification on compressor performance are given in the following paragraphs.

2702

Configuration A. - The redesigned compressor as received from the manufacturer was installed in the engine with the production outlet guide-vane assembly and the variable-area turbine-nozzle diaphragm.

Both the stage-pressure-ratio distributions (fig. 8) and the data of reference 1 indicate that satisfying radial equilibrium requirements in the inlet stages permitted a close approximation to design specifications.

Configuration B. - With the redesigned rotor, the first, second, and third stators were modified for configuration B as shown in table I. These stator changes combined with the angle settings of the first two redesigned rotors approach the simple radial equilibrium requirements in the inlet stages. The relatively small changes in performance affected by these modifications indicate that the rotor-angle changes approximated the desired flow conditions closely enough that the stator changes were unnecessary.

Configuration C. - With the stators of configuration B the ninth- and eleventh-stage rotor tips were twisted open 3° and 6°, respectively, in an attempt to satisfy more closely the radial equilibrium requirements in the exit stages. As has been pointed out in the section Compressor Modifications, such modifications might be expected to improve the low-speed performance of the compressor but to aggravate the high-speed surge problems. Thus configuration C provided an appreciable increase in the surge limit at equivalent speeds below 7800 rpm but had only a negligible effect on the surge limit above this speed. Although the surge pressure ratio at 7800 and 8000 rpm (fig. 10) is almost the same as for configuration A, the weight flow (fig. 11) has been increased slightly so that a plot of surge pressure ratio against weight flow would indicate a slightly reduced surge pressure ratio at a specified weight flow. At low speeds, however, the pressure ratio and weight flow are both increased so that the change in the surge line, on a pressure-ratio - weight-flow basis, would probably be negligible. Earlier investigations have proved that such modifications will result in slightly improved efficiencies at low speeds. Thus, the only benefits to be derived from configuration C would be a slight increase in efficiency or acceleration margin at low equivalent engine speeds. The decrease in surge-limit pressure ratio as a function of weight flow at speeds above design eliminated this configuration from consideration as an engine "fix." The fact that loading the tips of the ninth and eleventh rotors did not decrease the high-speed surge limit indicates that these sections were not critically loaded, and thus were not stalling, in the redesigned compressor (configuration A) at the high equivalent speeds. Because the performance at high speeds is practically unaffected by

these modifications, it appears that the tip sections of these rotors
are operating near the peak-pressure-ratio points of their section
performance curves, where changes in performance with angle of attack
are small.

Configuration D. - In configuration D, the ninth- and eleventh-
stage rotors were reset to the redesigned angles and the ninth- and
tenth-stage stators were closed 6° at the hub in order to unload the
last two compressor stages at high speed. This modification resulted
in a slight increase in the surge-limit pressure ratio over that of
configuration C at high equivalent speeds. However, at speeds of
7260 rpm and below, both the surge pressure ratio and the air weight
flow decreased appreciably. In general, this follows the trend
expected by unloading the exit stages of a compressor. The reduction
in the surge-limit pressure ratio at speeds below 7260 rpm appears
sufficient to reduce seriously the acceleration margin. This
modification combined with the ones in configurations C and E was
an attempt to determine whether the hub or tip sections of the exit
stages were most critical with respect to the high-speed surge line.

Configuration E. - The stators of configuration E were the same
as those of configuration B with the exception of the ninth and
tenth stages, which were closed 3° at both the hub and the tip section.
This modification unloaded the hub sections of the tenth and eleventh
rotors less than that of configuration D but also unloaded sections
near the tip slightly. Previous calculations have indicated that
resetting a row of stator blades a constant amount from hub to tip
alters the angle of attack on the following rotor more at the hub
than at the tip section.

This configuration (E) resulted in a small increase in the surge-
limit pressure ratio at speeds above 6000 rpm. The air flow increased
slightly at speeds of 7260 and 7800 rpm and decreased slightly at
8000 rpm. Although the low-speed surge line, on the basis of
pressure ratio against air flow, would be essentially unaltered, the
matching between the compressor and the turbine would be detrimentally
affected. The decrease in efficiency caused by such a modification
would be reflected in a reduction in the stable operating margin at
the reduced speeds. A comparison of configurations C, D, and E
indicates that the hub section of the exit stages is the most
critically loaded section at high equivalent speeds.

Configuration F. - For configuration F, a modified outlet guide-
vane assembly was installed in the engine with the redesigned rotor
and the stator vane assemblies of configuration B. The modified
outlet guide-vane assembly consisted of a standard outlet assembly
with alternate blades of the second blade row removed. This

modification was used to determine the effect of low solidity, and hence decreased resistance, on the high-speed surge limit. The investigation of reference 1 indicates that the mixer assembly effected an appreciable increase in the surge pressure ratio at high speed. The increase was believed due to a change in the resistance and effective volume of the system.

The effect of the reduced-solidity outlet guide vane can be determined by comparing configurations F with B and G with E. The net effect of the reduced-solidity, and hence reduced-flow resistance, outlet guide vanes depends on the flow distribution leaving the compressor. When used with the blading of configuration B, the reduced-solidity outlet vanes (configuration F) resulted in an increase in surge pressure ratio over the entire range of engine speeds.

Configuration G. - Configuration G was a rerun of configuration E with the standard outlet guide vanes replaced by the modified assembly. The purpose of this modification was to evaluate the effect of a low-solidity outlet on the high-speed surge limit. Both the surge-limit pressure ratio and the air flow were reduced over the entire speed range as compared with configuration E, except that the surge limit at 8000 rpm was unaffected.

Configuration H. - Configuration H is the same as configuration F with the exception of the inlet guide vanes which were opened 5°. As pointed out in the section Performance of Basic Redesign, the agreement between the design and actual pressure-ratio distributions within the compressor indicated that consideration of radial equilibrium and the loading of the first rotor hub were of primary importance. However, to prevent the hub section of the first rotor from turbining at speeds above design and to increase the air flow at high engine speeds, the inlet guide vanes were opened 5°, thus loading the first rotor hub still further. The effect of this modification was to increase the air flow appreciably at design speed and above, as compared with configuration F, and to increase the surge-limit pressure ratio at equivalent speeds above about 7600 rpm.

The effect on compressor performance of opening the inlet guide vanes is greater than any other modification and is in the desired direction. The improvement can be explained by considering the stage performance curves obtained from the interstage data for the first, fourth, eighth, and eleventh stages (fig. 12) and the calculations of the velocities after the inlet guide vanes for both the production and the opened vanes. In figure 12(a) data are presented giving the stage performance for stages 1, 4, 8, and 11 plotted as stage pressure coefficient $T_1 Y/U_t^2$ against the flow parameter $\dfrac{W_a \sqrt{\theta_1}/\delta_1}{U_t/\sqrt{\theta_1}}$ for

configuration E; and in figure 12(b) data are presented showing the
same parameters for configuration H. These parameters are discussed
and derived in detail in reference 3. They serve as a convenient
means of synthesizing the performance of any stage of a compressor
over a wide range of speeds. An exact evaluation of the effects of
the inlet-guide-vane adjustment alone would require a comparison of
configurations F and H. However, such a comparison could not be
obtained, because only limited interstage data were available for
configuration F. Inasmuch as the effects of all previous modifica-
tions are generally small, the comparison of configuration E with
configuration H is considered to give a reasonable indication of the
effect of the guide-vane adjustment.

Calculations of the velocity after the inlet guide vanes, based
on simple radial equilibrium and on the assumption that the air
leaves at the trailing-edge angle, indicate that the angle of attack
at the first rotor tip is practically unaffected by the inlet-guide-
vane resetting, largely because of the change in weight flow
accompanying the resetting. The hub section of configuration H,
however, is operating at an angle of attack approximately 4° greater
than that of configuration E at any given speed. This increased
loading may be observed by comparing the first-stage performance
curves of figures 12(a) and 12(b). At high equivalent engine speeds
(7100 to 8000 rpm) the first stage of configuration E (fig. 12(a)) is
operating at a pressure coefficient of approximately -0.5, which
indicates a turbining condition. Although part of this negative
pressure coefficient is due to pressure losses in the inlet duct
system and the inlet guide vanes, the losses are believed to be
small. Decreasing the guide-vane turning by 5° in configuration H
(fig. 12(b)) results in a pressure coefficient for this stage of
approximately 1.0 for speeds of 7200 to 8000 rpm. Thus the reduced
guide-vane turning has caused the first rotor hub section to change
from a negative pressure coefficient, or turbining condition, to a
positive coefficient or pressure-rise condition at high equivalent
speeds. In addition to the hub loading, the guide-vane modification
causes an increase in the tip relative Mach number. Thus, part of
the increase in pressure coefficient at the high speeds is due to
Mach number effect. The hub loading also causes the peak pressure
coefficient (which occurs at a speed of approximately 4500 rpm) of
the first stage to increase from approximately 1.5 (configuration E)
to 2.5 (configuration H). Adjustment of the inlet-guide-vane angle
increased the first-stage pressure ratio over the entire equivalent
speed range. The pressure coefficients of the fourth, eighth, and
eleventh stages for both configurations E and H remain almost the same.
Thus the increase in over-all compressor pressure ratio appears
principally due to the improvement in the first-stage performance.

2702

Another interesting point to be noted in the stage performance plots of figure 12 is that the fourth stage appears to be stalled at equivalent speeds below approximately 7000 rpm. Thus any low-speed surge problems could probably be attributed largely to stall in this stage or in neighboring stages of the compressor.

Evidence that the exit section of the compressor instigates the high-speed surge problems may be seen by inspection of the eighth- and eleventh-stage performance curves of figure 12(b). This is indicated by the peaking of the characteristic curves of these stages.

For configuration E (fig. 12(a)) the eighth stage appears to stall at equivalent speeds above approximately 7800 rpm and the eleventh stage at equivalent speeds above about 7900 rpm. For configuration H (fig. 12(b)) the eighth and eleventh stages appear to stall at equivalent engine speeds above approximately 7500 rpm. Exact determination of the stall speed is not possible because of the scatter of the data.

Configuration I. - The ninth- and tenth-stage stator changes of configuration D (unloading the tenth and eleventh rotor hubs) were incorporated with the opened inlet guide vanes of configuration H in an attempt to increase the surge limit still further (configuration I). By comparing the performance of configurations I with H and D with B, it may be seen in figures 10 and 11 that this modification had practically the same effect on the compressor with the modified inlet and outlet guide vanes as it had on the compressor with the production guide vanes.

Configuration J. - Configuration J is the same as configuration H with the exception of the outlet guide-vane assembly, which was replaced with the mixer assembly in order to evaluate the effect of the mixer on the surge limit. A comparison of the performance of configuration H with J indicated that the effect of the mixer is approximately the same as that reported in reference 1. Both the surge pressure ratio and the weight flow increased at high equivalent speeds, but the pressure ratio decreased at a speed of 6000 rpm. A similar effect was noted at high equivalent speeds when the solidity of the second row of outlet guide vanes was reduced by one half (configuration F), thus indicating that the resistance has a noticeable effect on the surge-limit pressure ratio.

Configuration K. - In configuration K the modified stators in the first, second, and third stages of configuration J were replaced with the production stator assemblies used in configuration A. This modification was made only to evaluate the relative merit of the modified and production stators, since a minimum number of blade

changes were desirable from a production standpoint. The effect of replacing the first three modified stator rows with production diaphragms was to increase the surge limit slightly at speeds above design and to decrease it slightly at design speed and below. The air flow decreased only slightly at 8000 rpm but decreased very appreciably at design speed. These results are consistent with those obtained with configurations B and A.

Configuration L. - Although it was realized that loading the exit stage might have a large detrimental effect on the high-speed surge condition, the eleventh rotor tip was twisted open 6° (configuration L) in an attempt to improve temperature distribution at the turbine inlet by improving the flow distribution out of the compressor. The production stators of stages 1, 2, and 3, which were used in configuration K, were replaced with the modified stators used first in configuration B. These modifications increased the surge-limit pressure ratio at design speed but seriously reduced both the surge limit and the weight flow at equivalent speeds above design, as would be expected for a stalled exit stage.

Configuration M. - The eleventh-stage rotor was reset to the redesigned section angle to recover the loss in surge pressure ratio caused by the preceding modification, and the variable-area turbine-nozzle diaphragm was replaced with the production turbine. This was the final configuration (M) and was used in the subsequent performance evaluation. As shown on the bar charts of figures 10 and 11, the surge-limit pressure ratios and air weight flows are the same as those of configuration J, although the surge limit of configuration M could not be obtained by steady-state operation, as in the other configurations, because of the fixed-area production turbine-nozzle diaphragm. Because the only difference between configurations J and M was the turbine-nozzle area, the compressor surge limits were presumed to be identical. Similarly, the weight-flow data obtained with configuration M were used to substantiate the limited air-flow data obtained with configuration J.

The surge-limit pressure ratio of the configuration M compressor is plotted as a function of equivalent engine speed in figure 13. Data were obtained for two different flight conditions, and the effect on the surge limit was negligible. For comparison the surge limit of the redesigned compressor (configuration A) is shown by the dashed line. It is evident that the modifications of configuration M substantially increased the high-speed surge limit over that of the redesigned compressor.

In addition to the surge limits, the military-rated operating lines (turbine-inlet temperature of 1885° R at an equivalent engine speed of 7260 rpm) of the respective configurations are also shown.

2702

Although the military-rated operating line of configuration A does not intersect the surge line in the range of engine speeds shown, the margin between them decreases rapidly at speeds above 8000 rpm. At inlet-air temperatures lower than about -60° F ($N/\sqrt{\theta}$ = 8300 rpm), compressor surge would probably be encountered and thus impose a thrust reduction on the engine. At inlet-air temperatures of approximately -32° F ($N/\sqrt{\theta}$ = 8000 rpm), the margin between the operating line and the surge limit may be insufficient to prevent compressor surge when transient disturbances, such as lighting an afterburner, are imposed on the engine. Configuration M eliminates this adverse relation because of the substantial increase obtained in the margin between the military-rated operating line and the surge limit.

Compressor Performance Maps

Pending sea-level static performance tests by the manufacturer, the engine herein with the configuration M compressor and an afterburner is considered to be a prototype of the J40-WE-8 turbojet engine. Consequently, the performance of this prototype engine without afterburner was extensively evaluated over a wide range of flight conditions and engine speeds for five fixed positions of the variable-area exhaust nozzle. The data of this evaluation were used to construct the compressor performance maps shown in figure 14 for a flight Mach number of 0.64 at altitudes of 15,000, 35,000, and 45,000 feet and for a flight Mach number of 1.00 at an altitude of 35,000 feet. In each map the surge limit was determined by extrapolating curves of constant speed from the steady-state operating lines to the surge-limit pressure ratio at that particular speed. Constant-speed lines and efficiency contours were determined by cross-plotting data obtained over a range of engine speeds for several fixed positions of the variable-area exhaust nozzle. Although good agreement of the surge limits on a weight-flow basis was obtained for each flight condition, the precise location of the surge limit may be questionable because of the large extrapolation required from the pressure ratio obtained with the smallest exhaust nozzle to the surge-limit pressure ratio. Operating lines for five fixed positions of the variable-area exhaust nozzle are superimposed on each compressor map.

It may be noted in figure 14 that the region of maximum compressor efficiency lies appreciably below the surge limit for all flight conditions. This characteristic is unusual in that peak efficiencies for most full-scale compressors are obtained much closer to the surge limit (references 4 to 6). At 15,000 feet a peak efficiency of 0.85 occurred at equivalent engine speeds between approximately 67 and 98 percent of rated speed. As the altitude was increased to 35,000 feet, the region in which the efficiency remained above 0.85 extended over a smaller speed range. At 45,000 feet (fig. 14(c))

the peak efficiency dropped slightly to 0.84 and extended over a still
smaller speed range. Thus it appears that as the Reynolds number
decreased (as altitude increased) the region of peak efficiency moved
to progressively higher equivalent speeds while the value of peak
efficiency decreased slightly. The effect of decreasing efficiency
on the performance was to shift the engine operating line for a given
exhaust-nozzle area upward with respect to the surge limit. Thus, for
a particular engine speed, the acceleration margin is decreased at
high altitude, even though the surge-limit pressure ratio remains
essentially constant with altitude.

The effect of increasing the flight Mach number from 0.64 to 1.00
at an altitude of 35,000 feet may be seen by comparing the performance
maps of figures 14(b) and 14(d). The region of maximum compressor
efficiency decreased to a smaller speed range and the engine operating
lines were moved to lower compressor pressure ratios. As a result, the
optimum-size exhaust nozzle, with respect to peak compressor efficiency,
decreased; and the acceleration margin increased.

Effect of Final Configuration on Engine Performance

The effect of the configuration M compressor modifications on the
performance of the redesigned compressor (configuration A) is shown in
figure 15(a). Ratios of net thrust and air flow are plotted against
equivalent engine speed for configuration M compared with configura-
tion A. Both net thrust and air flow were increased approximately
5 percent. The increase in thrust is primarily due to the increase
in air flow which resulted from opening the inlet guide vanes 5°.

The combined effects of the basic redesigned compressor and the
additional configuration M modifications on the performance of the
original production engine are shown in figure 15(b). Ratios of net
thrust and air flow are plotted against equivalent engine speed for
the final configuration (M) of this report compared with the original
production engine (reference 1). At an equivalent engine speed of
7260 rpm (sea level rated), the over-all increase in thrust is only
about 1 percent, which is primarily due to an equivalent increase in
air flow. However, at higher equivalent speeds the thrust ratio
increases rapidly primarily because of the removal of the compressor
surge limitation which had penalized the performance of the original
engine. Thus, at an equivalent engine speed of 8000 rpm the thrust
of configuration M is approximately 20 percent greater than that of
the original engine.

CONCLUDING REMARKS

The results of the investigation presented in this report have shown that a basically redesigned compressor to satisfy more closely simple radial equilibrium requirements in the inlet and exit stages markedly increased the compressor surge limit of the original XJ40-WE-6 engine at high equivalent speeds. The use of a mixer assembly at the compressor discharge also increased the surge limit slightly with no noticeable effect on the thrust. Opening the inlet guide vanes 5° increased the air flow about 5 percent above that of the basic redesigned compressor and resulted in approximately the same increase in thrust.

Complete compressor performance maps of the final configuration were obtained for four different flight conditions. Altitude and flight Mach number had little effect on the compressor surge limit, but a slight drop in efficiency due to Reynolds number effect decreased the acceleration margin slightly at high altitudes.

Lewis Flight Propulsion Laboratory
    National Advisory Committee for Aeronautics
        Cleveland, Ohio

APPENDIX A

SYMBOLS

The following symbols are used in this report:

$c_{p,a}$ specific heat of air, 0.24 Btu/(lb)($^\circ$F)

$c_{p,g}$ specific heat of exhaust gas, Btu/(lb)($^\circ$F)

F_n net thrust, lb

f/a fuel-air ratio

g gravitational constant, 32.2 ft/sec^2

K, K' constants

N engine rotational speed, rpm

$N/\sqrt{\theta}$ sea-level equivalent speed, rpm

P total pressure, lb/sq ft abs

p_0 ambient altitude pressure, lb/sq ft abs

r radius, in.

T total temperature, $^\circ$R

T/θ sea-level equivalent total temperature, $^\circ$R

U blade speed, ft/sec

$V_{j,eff}$ effective jet velocity, ft/sec

V_0 flight speed, ft/sec

W_a air weight flow, lb/sec

W_g exhaust-gas weight flow, $W_a(1 + f/a)$, lb/sec

$W\sqrt{\theta}/\delta$ sea-level equivalent weight flow, lb/sec

Y pressure function $\left[\left(\dfrac{P_o}{P_i}\right)^{\frac{\gamma-1}{\gamma}} - 1\right]$

γ isentropic exponent

γ_a ratio of specific heat for air

γ_g ratio of specific heat for exhaust gas

Δh_c enthalpy rise through compressor, Btu/lb

Δh_t enthalpy drop through turbine, Btu/lb

δ ratio of total pressure to standard sea-level pressure

η_c compressor adiabatic efficiency

η_t turbine adiabatic efficiency

θ ratio of total temperature to standard sea-level temperature

Subscripts:

a   air

c   compressor

g   exhaust gas

i   inlet of stage or section

j   jet

n   net

o   outlet of stage or section

t   rotor tip section, turbine

O   ambient

1   cowl inlet

2   engine inlet

3   compressor inlet

4   compressor discharge

5   turbine inlet

6   turbine outlet

7   exhaust nozzle

2702

APPENDIX B

CALCULATION OF IDEAL NET THRUST

During initial performance tests of the original configuration, unexpected compressor surge at high equivalent engine speeds resulted in minor damage to the tunnel scales. Hence the thrust readings could not be considered reliable. In later tests of other configurations, thrust data were not obtained at rated conditions because limiting turbine-inlet temperatures could not be maintained.

In order to compare impartially the performance of various configurations at rated conditions, it was necessary to rely on calculated values of net thrust. Although the magnitude of such calculated thrusts may be slightly in error, the use of ratios for a comparison is reliable. A further check of the calculated thrusts was made by extrapolating the altitude performance data to limiting turbine temperatures. The calculated values agreed with the extrapolated experimental data within 3 percent.

Net-thrust ratios of the final configuration (M) to the redesigned compressor (configuration A) and of the final configuration (M) to the original production engine (reference 1) are presented in figures 15(a) and 15(b), respectively. The values of ideal net thrust used in this figure were obtained by the following method of calculation.

By assuming choked flow through the turbine for equivalent engine speeds greater than 7000 rpm, the continuity equation may be used to obtain the following relation:

$$\frac{\dfrac{W_a\sqrt{\theta}}{\delta}\sqrt{\dfrac{T_5}{\theta}}}{\left(\dfrac{P_5}{P_2}\right)} = K' \tag{1}$$

If the pressure drop through the combustion chamber is considered constant, equation (1) may be expressed in terms of equivalent air weight flow, turbine-inlet temperature, and compressor pressure ratio as

$$\frac{\dfrac{W_a\sqrt{\theta}}{\delta}\sqrt{\dfrac{T_5}{\theta}}}{\left(\dfrac{P_4}{P_2}\right)} = K \tag{2}$$

Since engine performance is evaluated from station 2 (engine inlet), the compressor pressure ratio is considered to be from station 2 to station 4.

An average value of the constant K was determined from experimental data obtained at several high equivalent engine speeds. At actual rated engine speed N of 7260 rpm, θ was calculated for equivalent engine speeds $N/\sqrt{\theta}$ of 7000, 7200, 7400, 7600, 7800, and 8000 rpm. Values of equivalent weight flow $W_a\sqrt{\theta}/\delta$ at the above equivalent engine speeds were obtained from faired curves of experimental data. The turbine-inlet temperature T_5 was assumed limiting at 1885° R (manufacturer's specification), and the compressor pressure ratio P_4/P_2 was calculated from equation (2).

With the pressure ratio known, the actual work of compression per unit weight flow may be calculated from

$$\Delta h_c = \frac{c_{p,a}T_2\left[\left(\dfrac{P_4}{P_2}\right)^{\frac{\gamma_a - 1}{\gamma_a}} - 1\right]}{\eta_c} \tag{3}$$

where compressor efficiency η_c is obtained from experimental data.

With the enthalpy rise across the compressor assumed equal to the enthalpy drop across the turbine, the turbine-outlet temperature T_6 may be calculated from

$$\Delta h_c = \Delta h_t = \frac{W_g}{W_a}\, c_{p,g}(T_5 - T_6) \tag{4}$$

where $W_g/W_a = (1 + f/a)$ and the fuel-air ratio is assumed equal to 0.015.

The turbine-outlet total pressure P_6 may then be calculated as follows:

$$P_6 = P_5\left(1 - \frac{1 - \dfrac{T_6}{T_5}}{\eta_t}\right)^{\frac{\gamma_g}{\gamma_g - 1}} \tag{5}$$

where the turbine efficiency η_t is obtained from experimental data, and the turbine-inlet total pressure P_5 is assumed to be 95 percent

2702

of compressor-discharge total pressure. From P_6, the effective jet velocity $V_{j,eff}$ was calculated with an ambient altitude pressure p_0 (628 lb/sq ft abs at 30,000 ft) for a γ_g of 1.3.

The actual weight flow W_a was calculated from the equivalent weight flow $W_a\sqrt{\theta}/\delta$, where δ corresponds to engine-inlet conditions at a flight Mach number of 0.64 at an altitude of 30,000 feet; and θ was determined at an actual engine speed of 7260 rpm for sea-level equivalent engine speeds of 7000, 7200, 7400, 7600, 7800, and 8000 rpm.

The net thrust was then calculated by subtracting inlet momentum from the jet thrust

$$F_n = \frac{W_g V_{j,eff}}{g} - \frac{W_a V_0}{g}$$

REFERENCES

1. Finger, Harold B., Essig, Robert H., Conrad, E. William: Effect of Rotor- and Stator-Blade Modifications on Surge Performance of an 11-Stage Axial-Flow Compressor. I - Original Production Compressor of XJ40-WE-6 Engine. NACA RM E52G03, 1953.

2. Allen, Sydney, and Hamm, J. R.: A Pyrometer for Measuring Total Temperature in Low-Density Gas Streams. A.S.M.E. Trans., vol. 72, no. 6, Aug. 1950, pp. 851-858.

3. Finger, Harold B., and Dugan, James F., Jr.: Analysis of Stage Matching and Off-Design Performance of Multistage Axial-Flow Compressors. NACA RM E52D07, 1952.

4. Medeiros, Arthur A., Guentert, Donald C., and Hatch, James E.: Performance of J35-A-23 Compressor. I - Over-All Performance Characteristics at Equivalent Speeds from 20 to 100 Percent of Design. NACA RM E50J17, 1951.

5. McAulay, John E., Sobolewski, Adam E., and Smith, Ivan D.: Performance of the Components of the XJ34-WE-32 Turbojet Engine over a Range of Engine and Flight Conditions. NACA RM E51L10, 1952.

6. Budinger, Ray E., and Thomson, Arthur R.: Investigation of NACA 10-Stage Subsonic Axial-Flow Compressor. II - Preliminary Analysis of Over-All Performance. NACA RM E52C04, 1952.

TABLE I - ENGINE CONFIGURATIONS

[Redesign, basic redesign of original production compressor; M, modified by removal of alternate blades in second row; P, production; V. A., variable area]
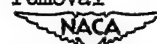
Config-uration	Compressor stages 1 to 10		Outlet guide-vane assembly	1st-stage turbine diaphragm	Inlet guide vanes
	Rotors	Stators			
A	Redesign	Production	P	V.A.	P
[a]B	Redesign	Stage Hub Mean Tip 1 1.8 -2.5 -3.4 2 .3 - .2 -2.0 3 -1.6 1.6 -2.3	P	V.A.	P
C	Open 11th rotor 6° at tip Open 9th rotor 3° at tip	Same as B	P	V.A.	P
D	Redesign	Same as B except 9th- and 10th-stage stators closed 6° at hub. No change at tip.	P	V.A.	P
E	Redesign	Same as B except 9th- and 10th-stage stators closed 3° at both tip and hub.	P	V.A.	P
F	Redesign	Same as B	M	V.A.	P
G	Redesign	Same as E	M	V.A.	P
H	Redesign	Same as B	M	V.A.	Open 5°
I	Redesign	Same as D	M	V.A.	Open 5°
J	Redesign	Same as B	Mixer	V.A.	Open 5°
K	Redesign	Production	Mixer	V.A.	Open 5°
L	Open 11th rotor 6° at tip	Same as B	Mixer	V.A.	Open 5°
M	Redesign	Same as B	Mixer	P	Open 5°

[a]Negative angles indicate decreasing angle between blade chord and tangential direction.
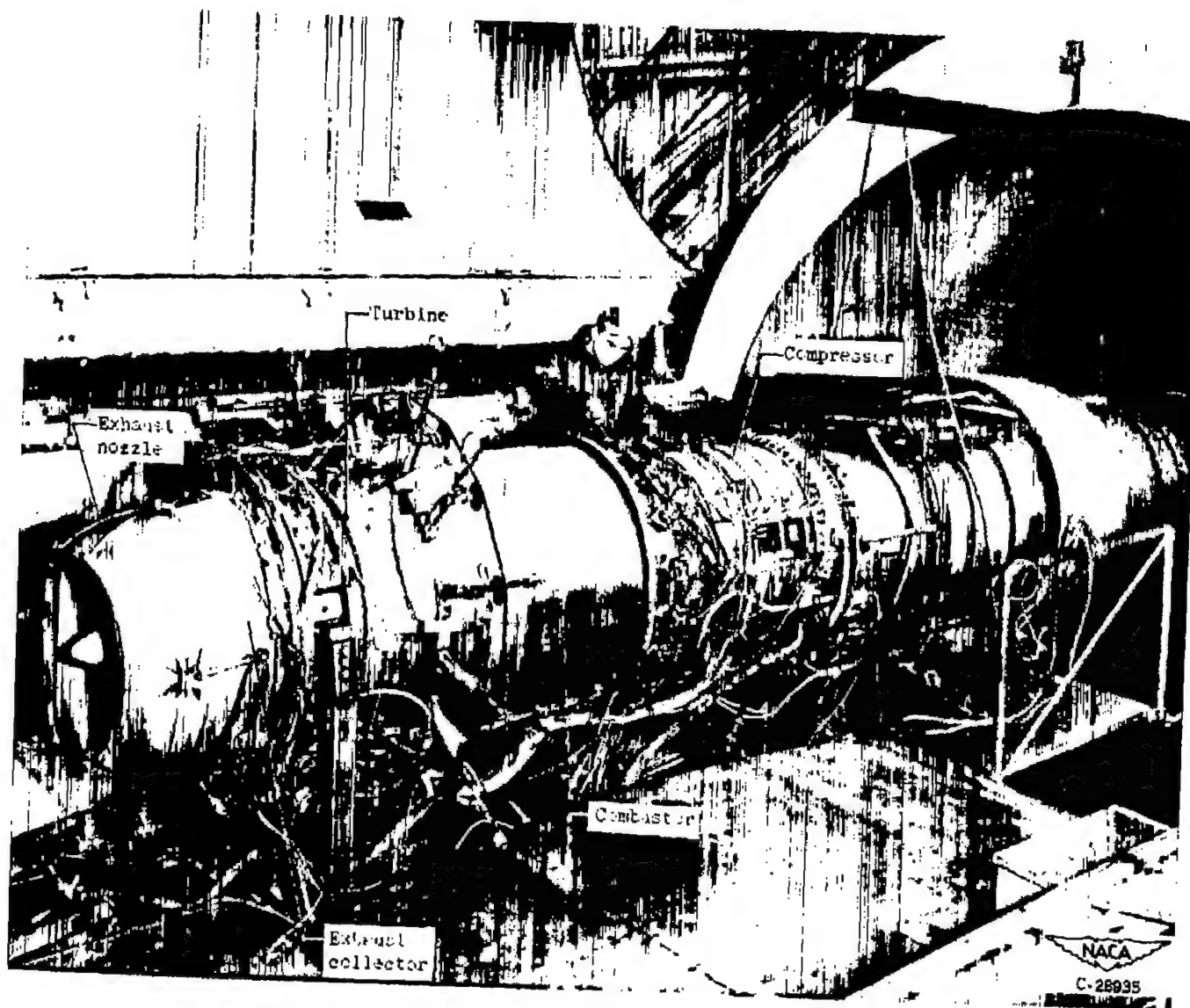
Figure 1. - XJ40-WE-6 engine installed in altitude wind tunnel.
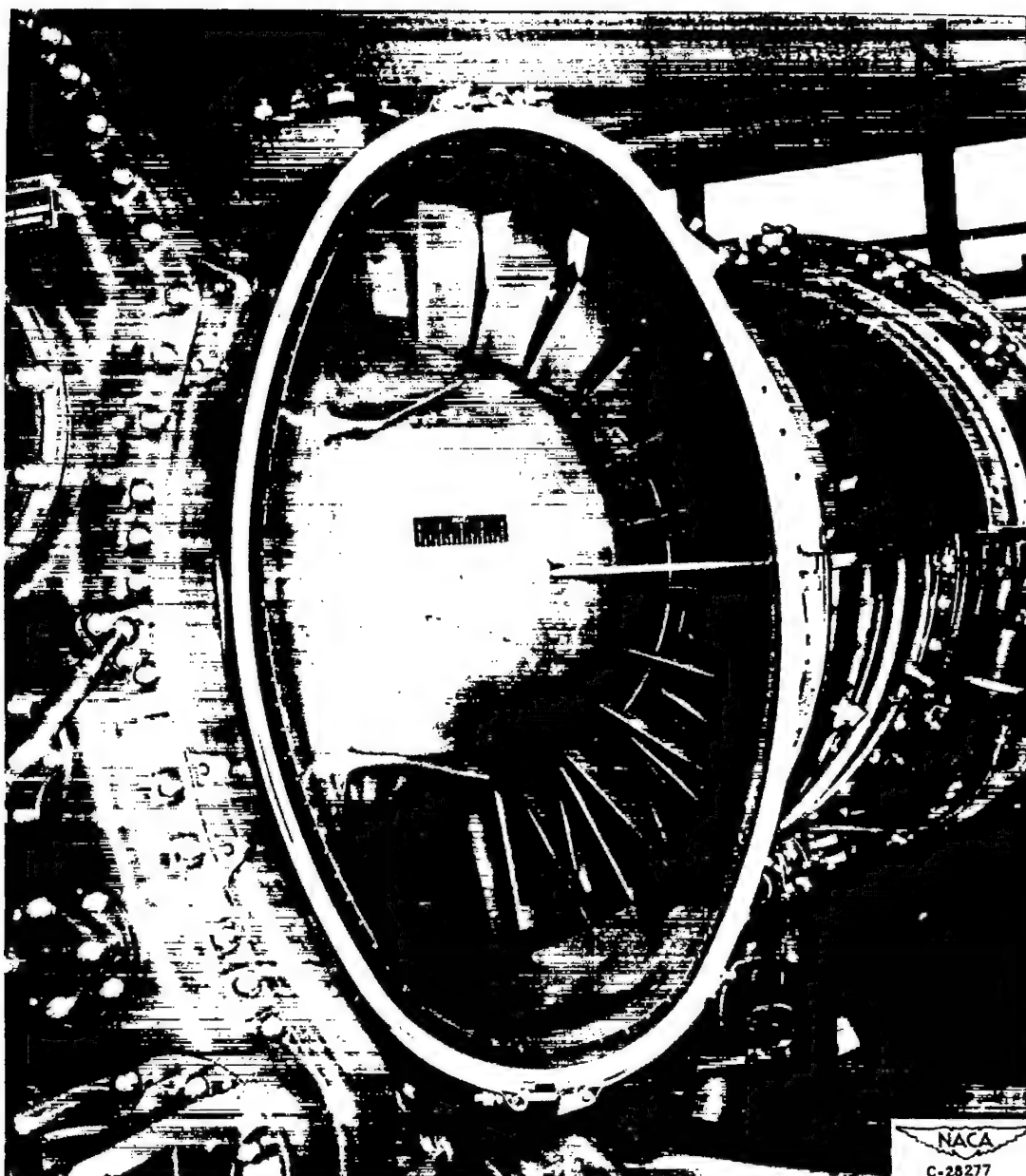
Figure 2. - Compressor-inlet duct section.
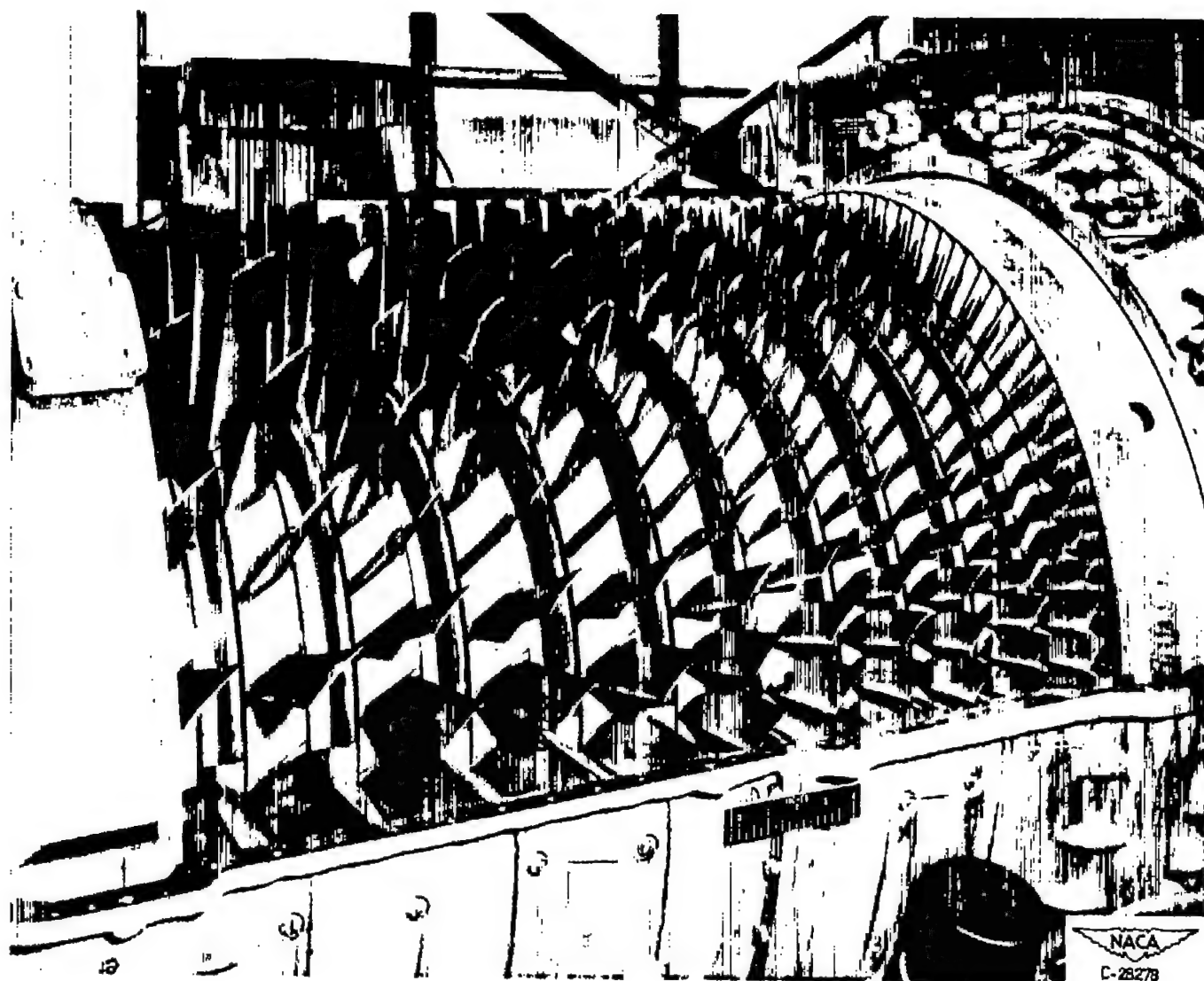
Figure 3. - View of compressor with top half of casing removed.

Main actuating shaft

Engine outer skin

Nozzle actuating ring

Nozzle actuating arm

Roller

Turbine-inlet-annulus outer skin

Variable-area turbine-nozzle vane

Turbine-inlet-annulus inner skin
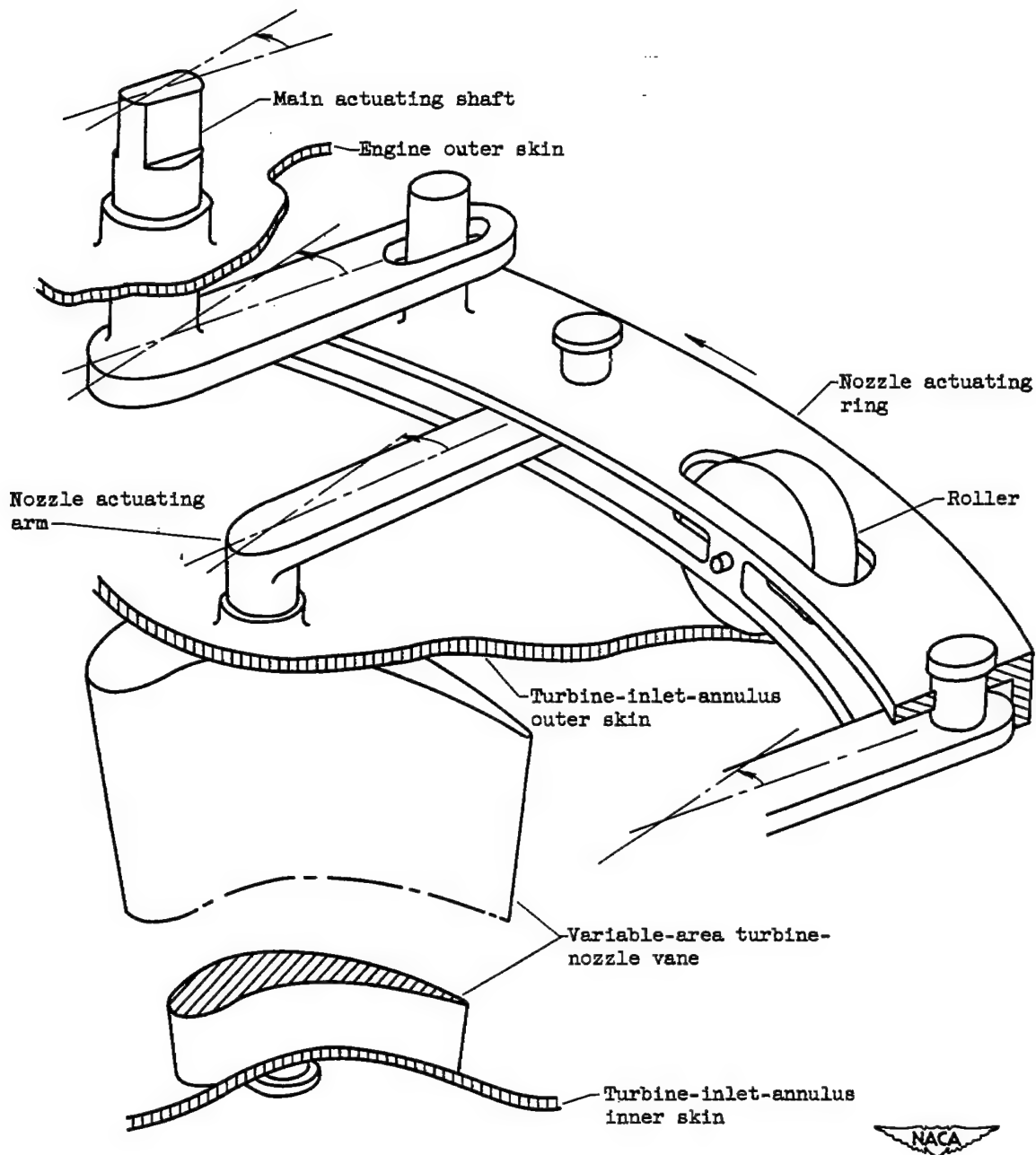
Figure 4. - Schematic sketch of variable-area turbine-nozzle actuating mechanism.

Interstage
survey
stations
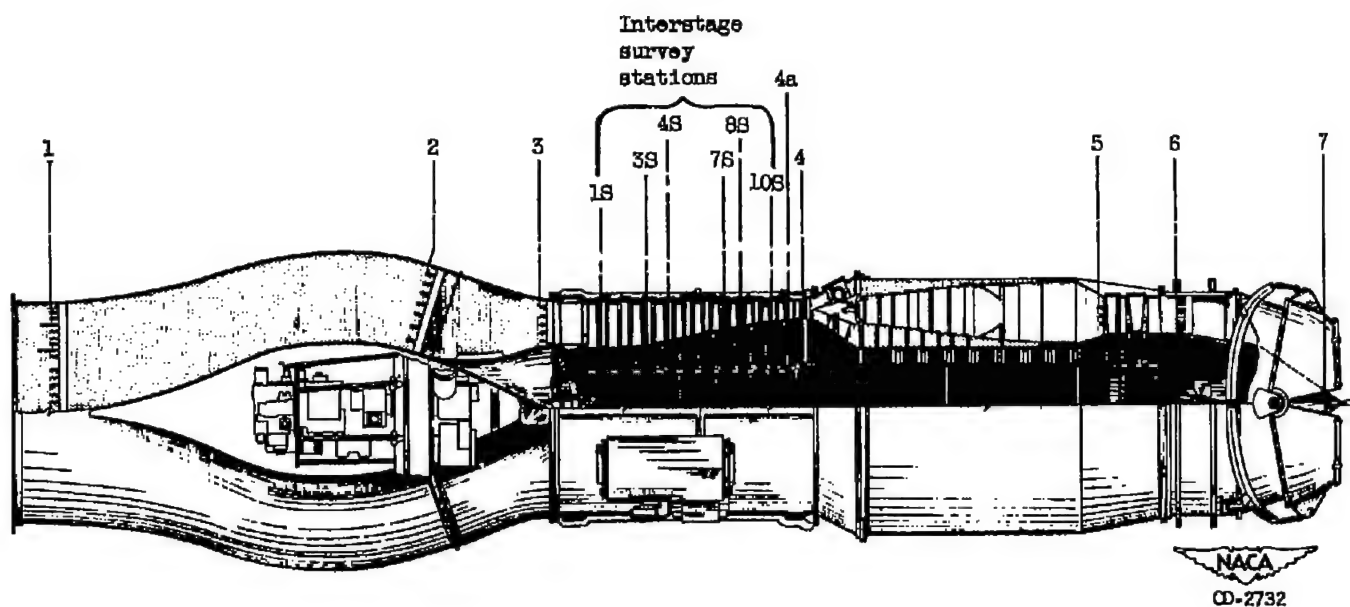
Figure 5. – Cross-section drawing of engine showing instrument stations.
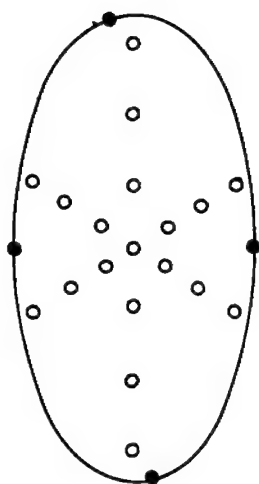
Station 2
Engine inlet
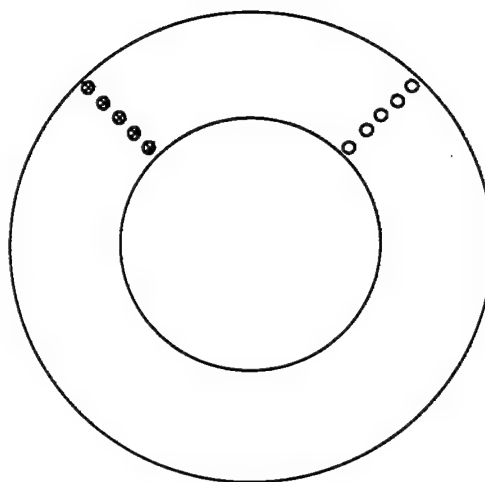
Typical interstage station

o Total pressure
e Temperature
● Static pressure
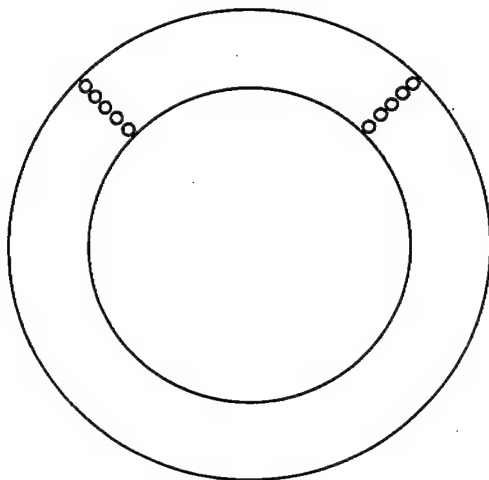
Station 4a
Inlet to 11th-stage stator
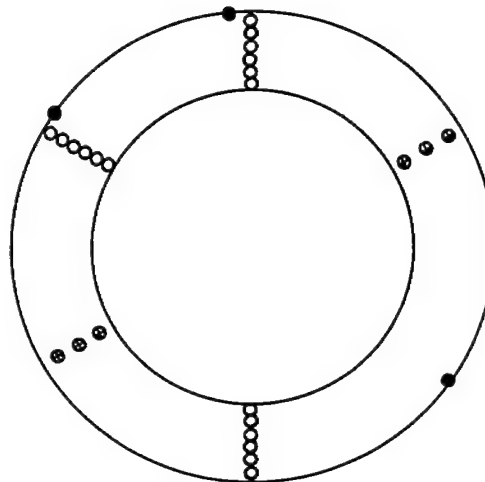
Station 4
Compressor discharge

Figure 6. - Schematic diagram showing location of instrumentation
at several compressor stations.
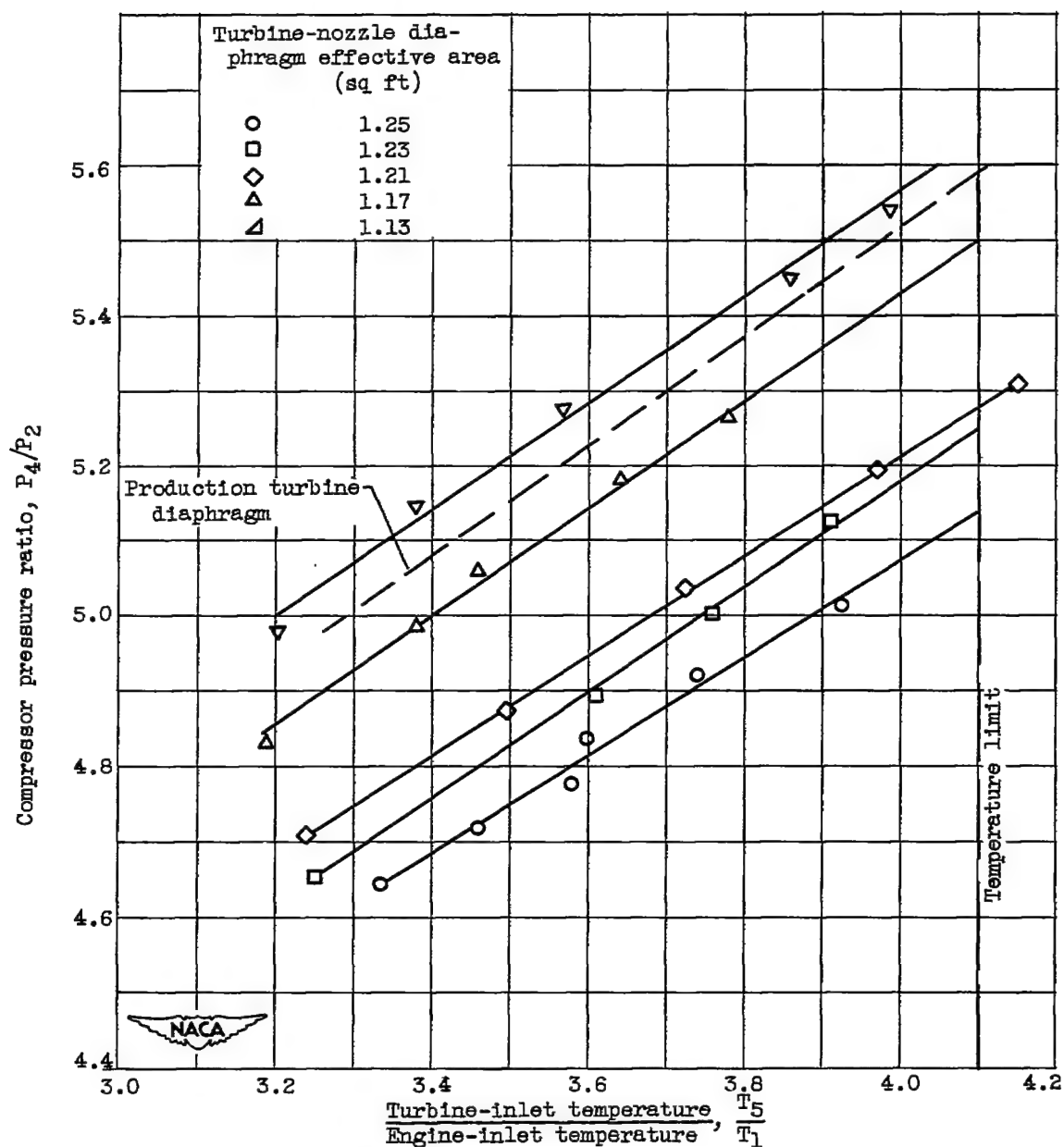
Figure 7. - Effect of changing turbine-nozzle-diaphragm area on compressor pressure ratio at a pressure altitude of 30,000 feet, flight Mach number of 0.62, and equivalent engine speed of 7710 rpm.
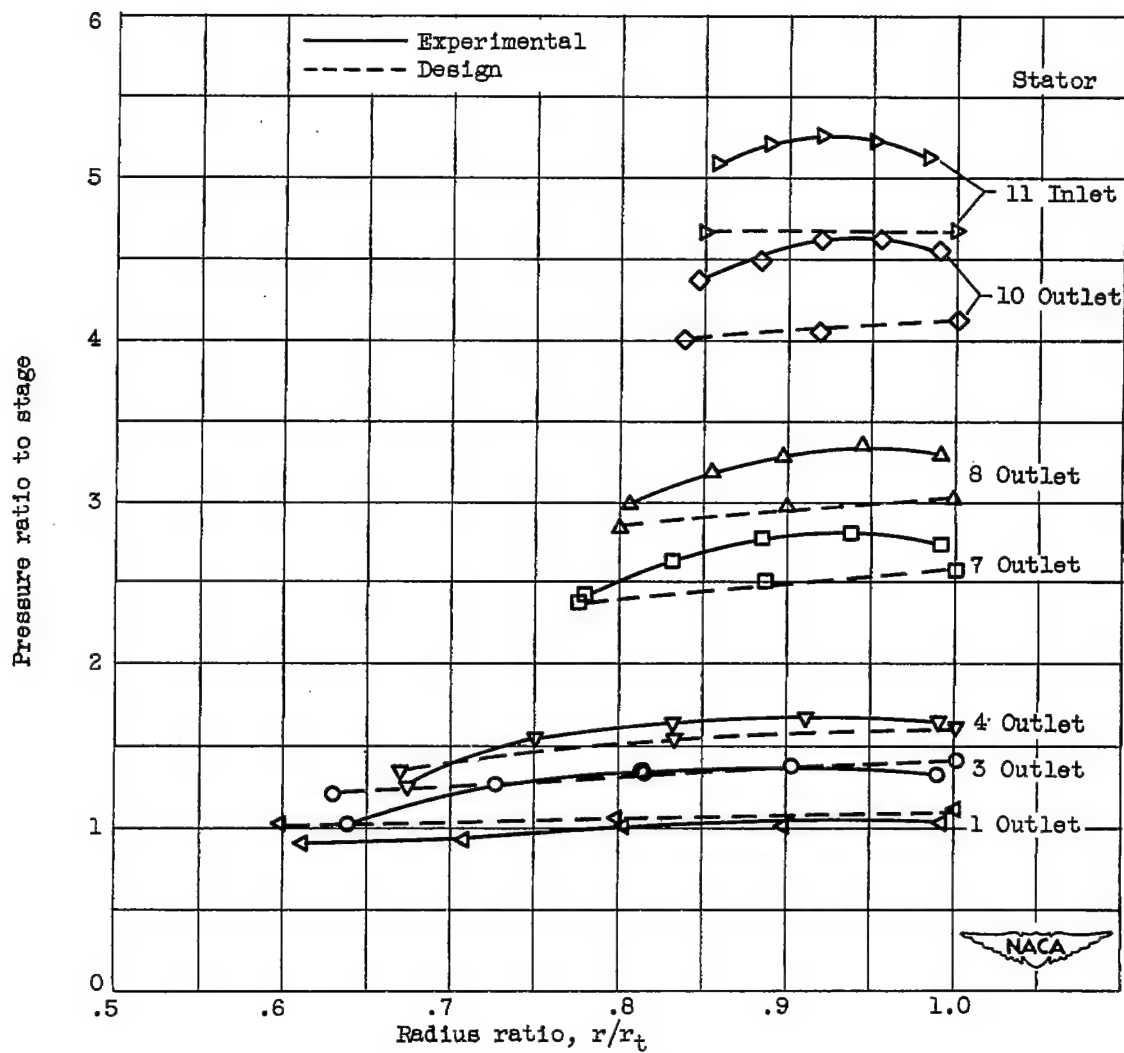
Figure 8. - Total-pressure-ratio distributions at several stator stations of redesigned compressor (configuration A) at an equivalent engine speed of 7253 rpm.
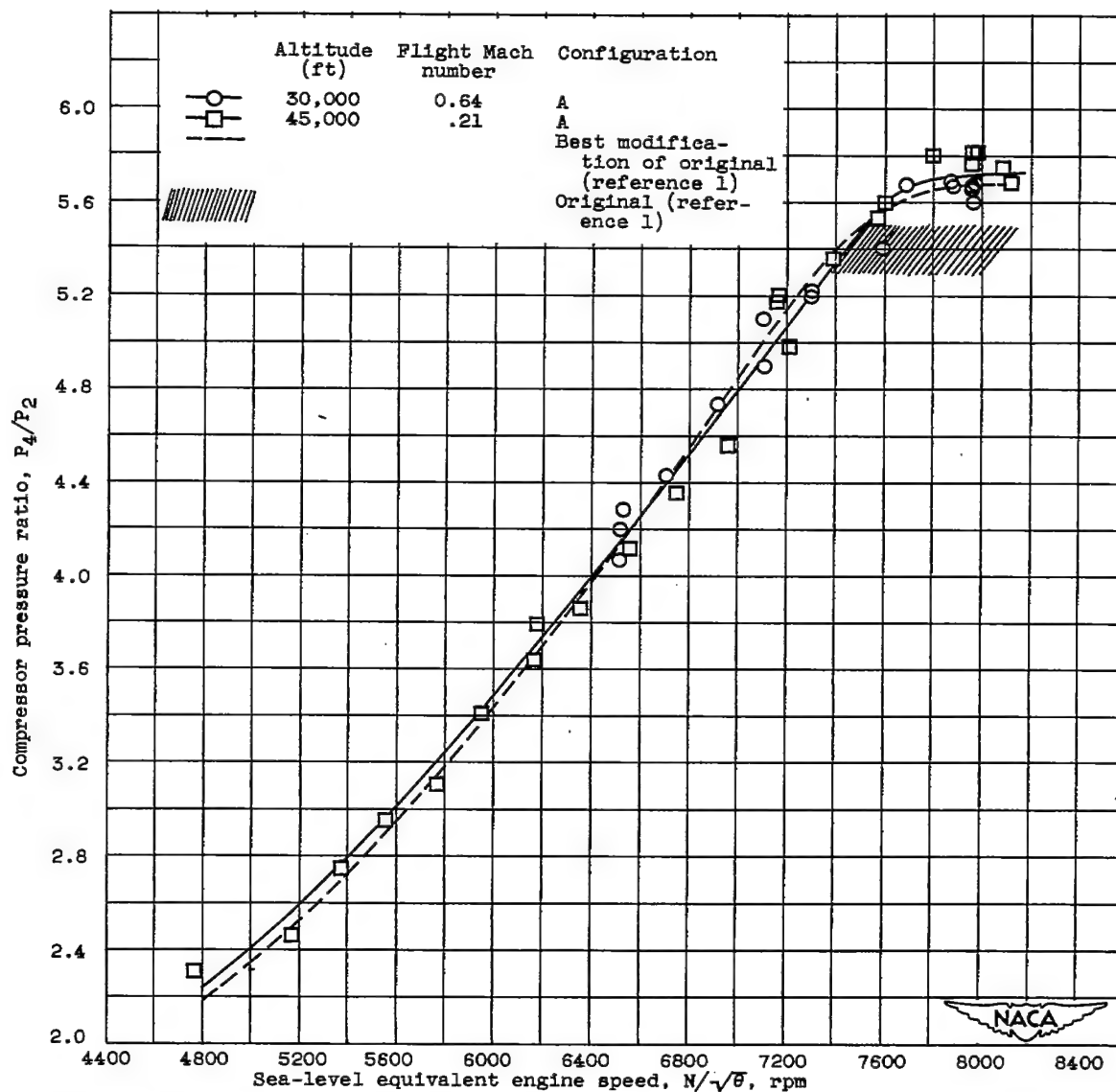
Figure 9. - Surge limit of redesigned compressor (configuration A) compared with original compressor and best modification of original compressor (reference 1).

2702
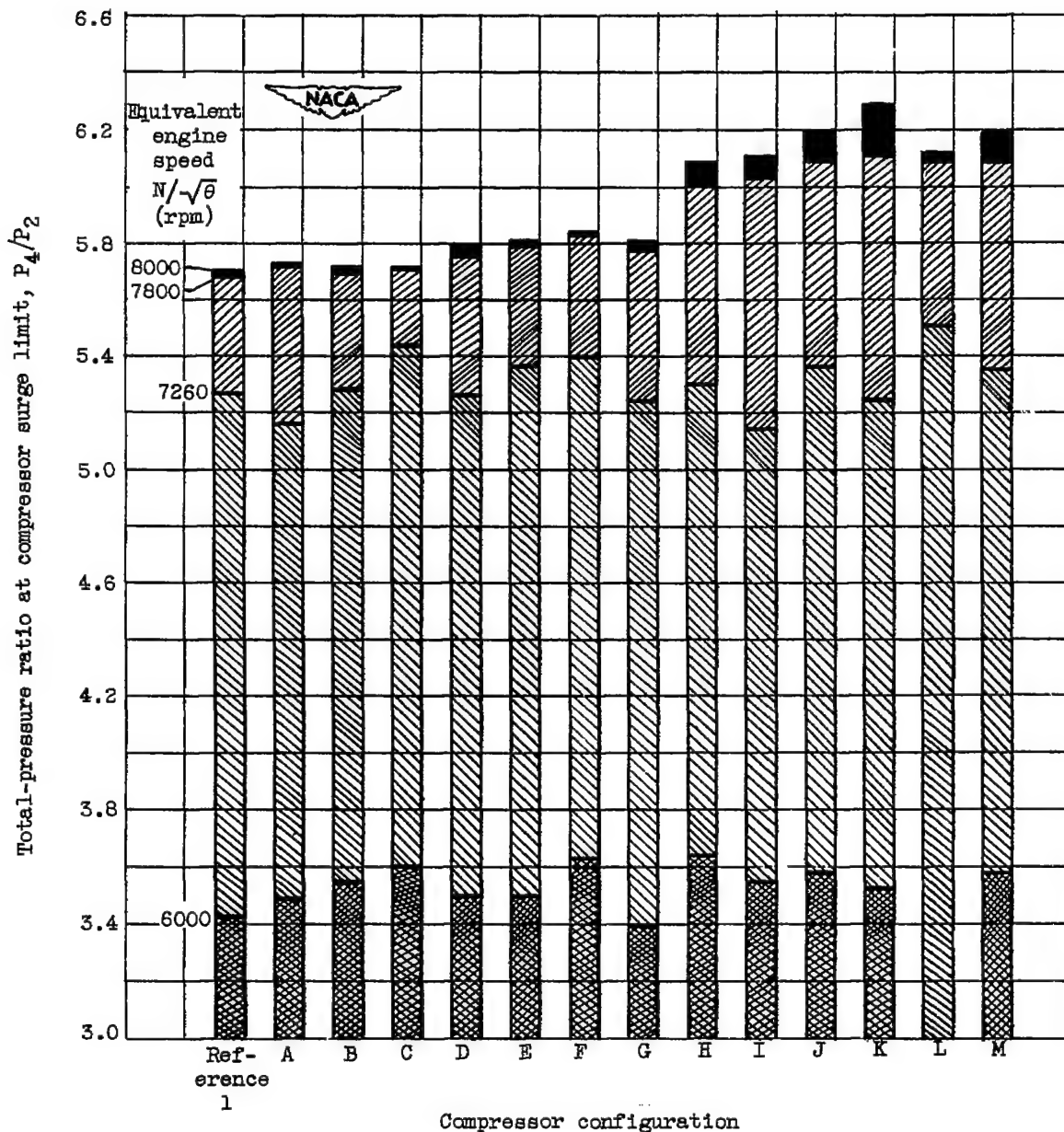
Figure 10. - Surge-limit pressure ratios of various compressor configurations. Altitude, 30,000 feet; flight Mach number, 0.64. Surge-limit pressure ratio for configuration L not obtained at an equivalent engine speed of 6000 rpm.
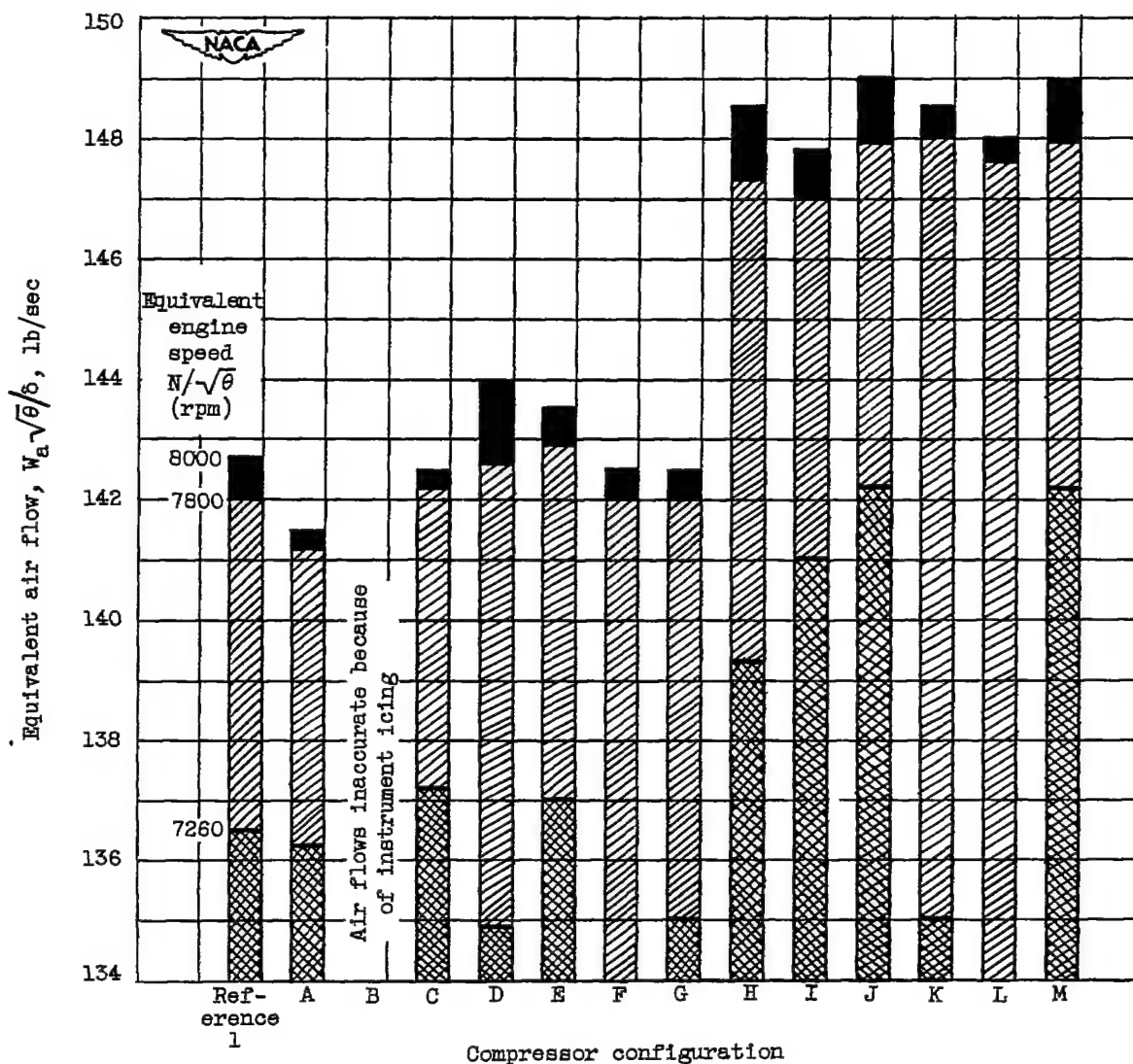
Figure 11. - Equivalent air flows of various compressor configurations. Altitude, 30,000 feet; flight Mach number, 0.64. Weight flows for configurations F and L not obtained for equivalent engine speeds below 7800 rpm.
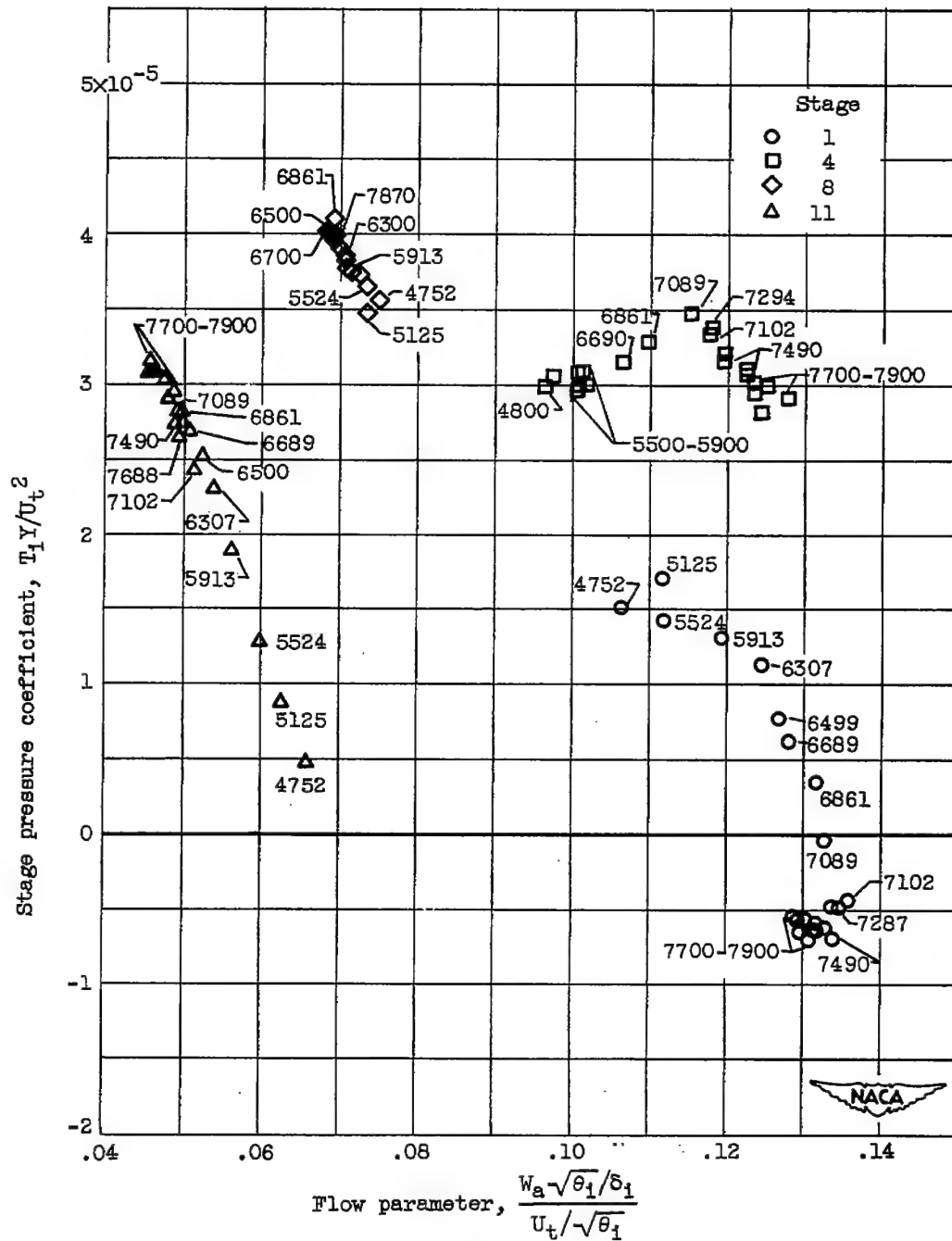
(a) Configuration E.

Figure 12. - Stage operating points for several stages of XJ40-WE-6 compressor for various equivalent engine speeds.

CONFIDENTIAL

2702
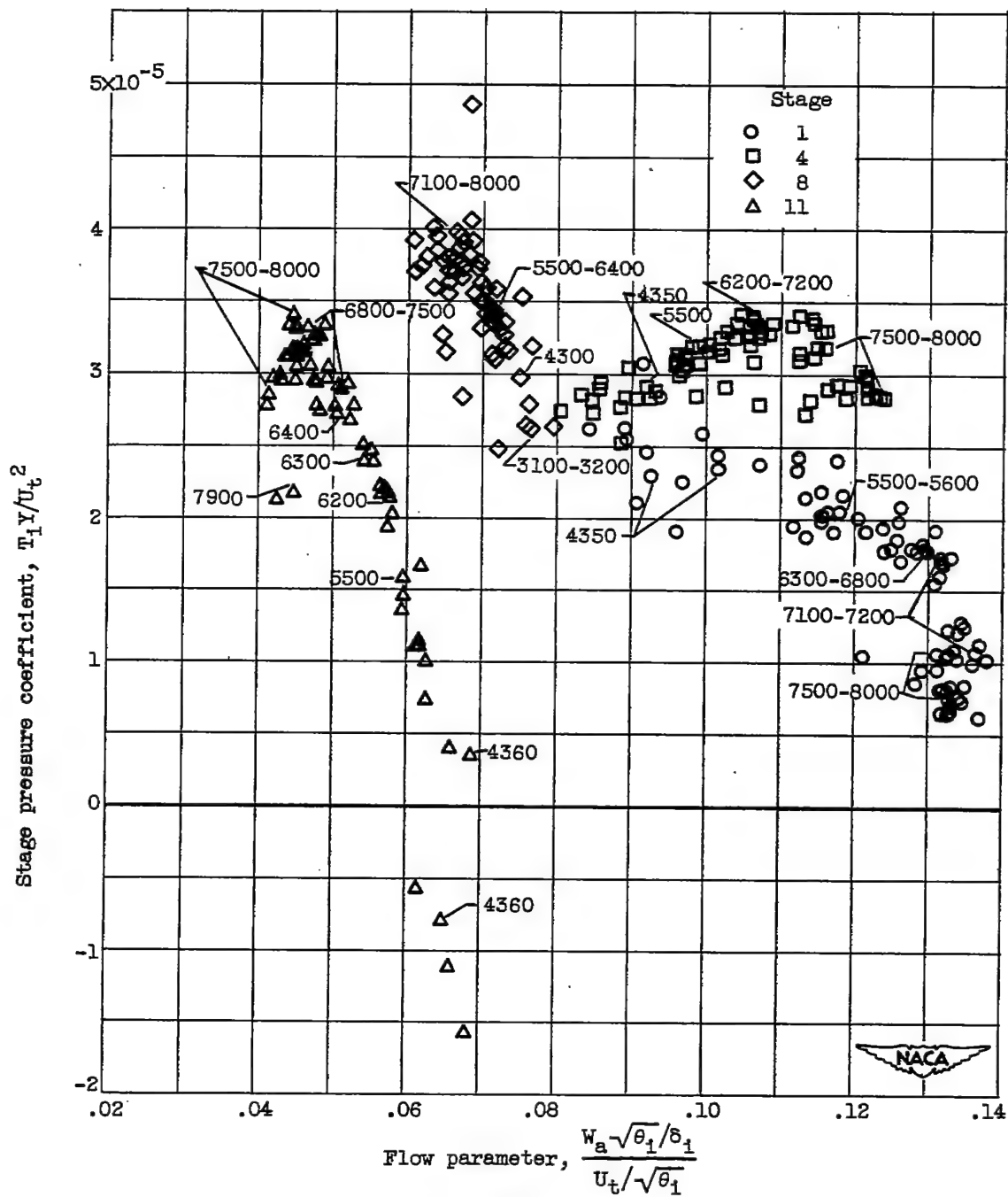
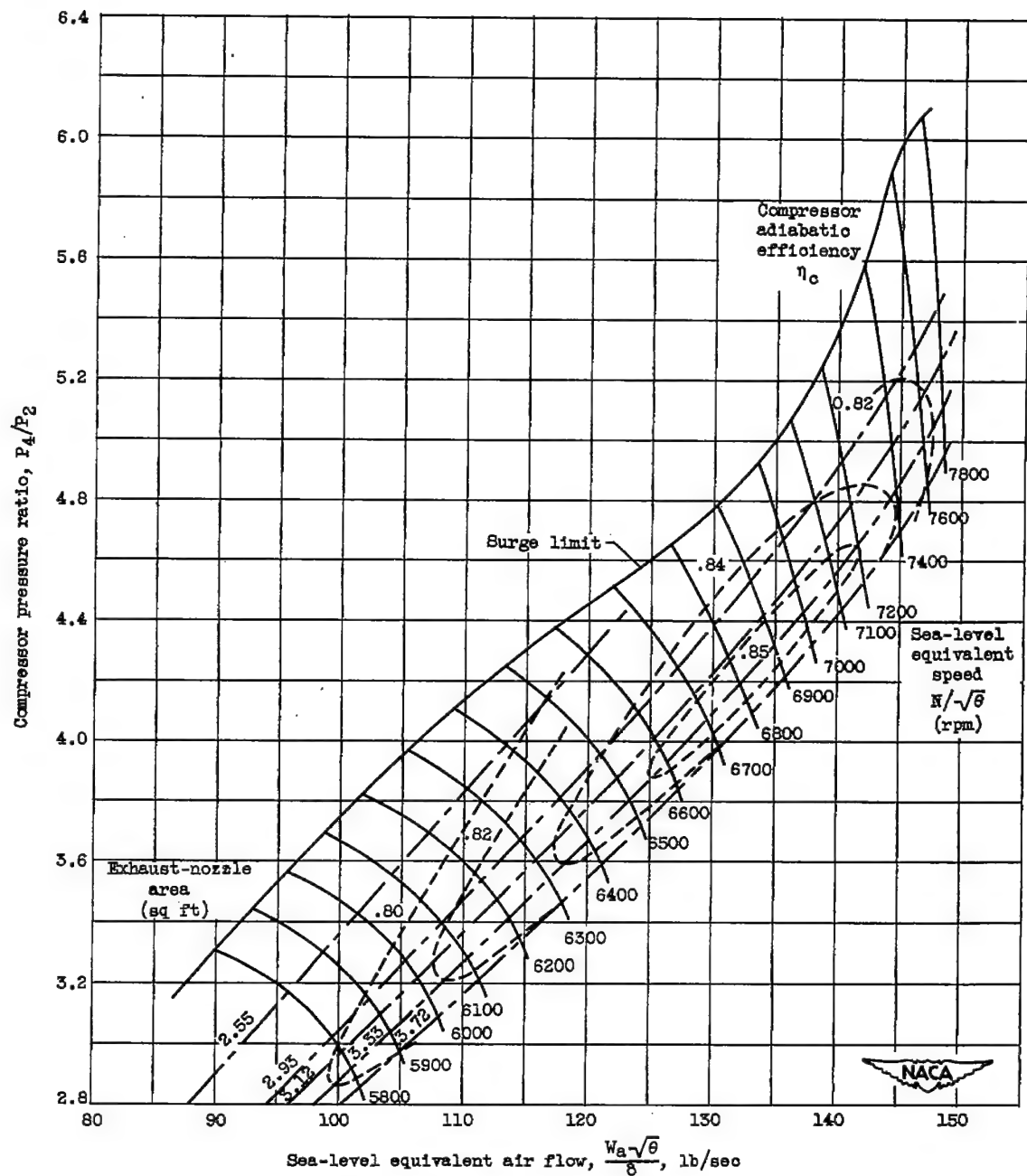(b) Configuration H.

Figure 12. - Concluded. Stage operating points for several stages of XJ40-WE-6 compressor for various equivalent engine speeds.
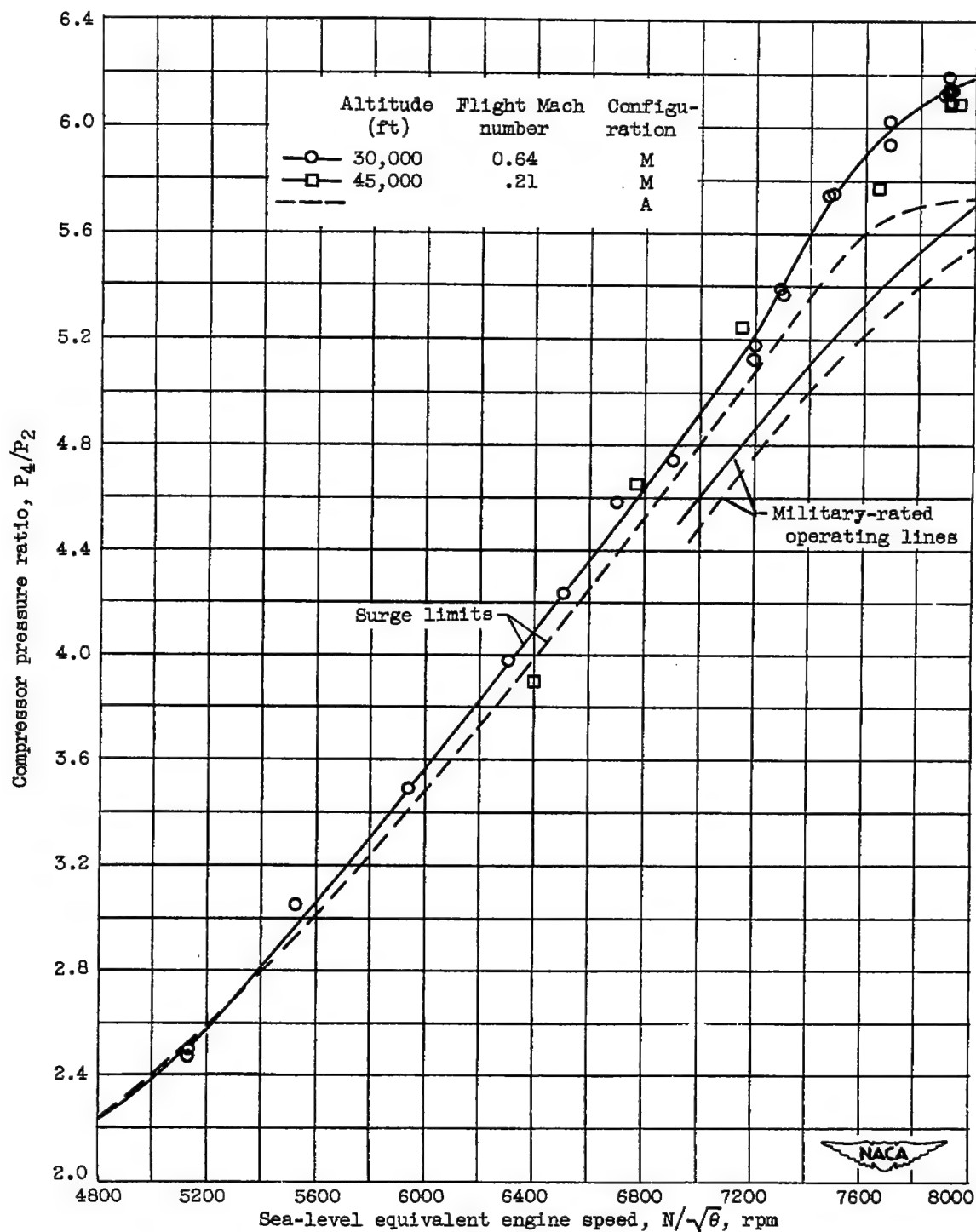
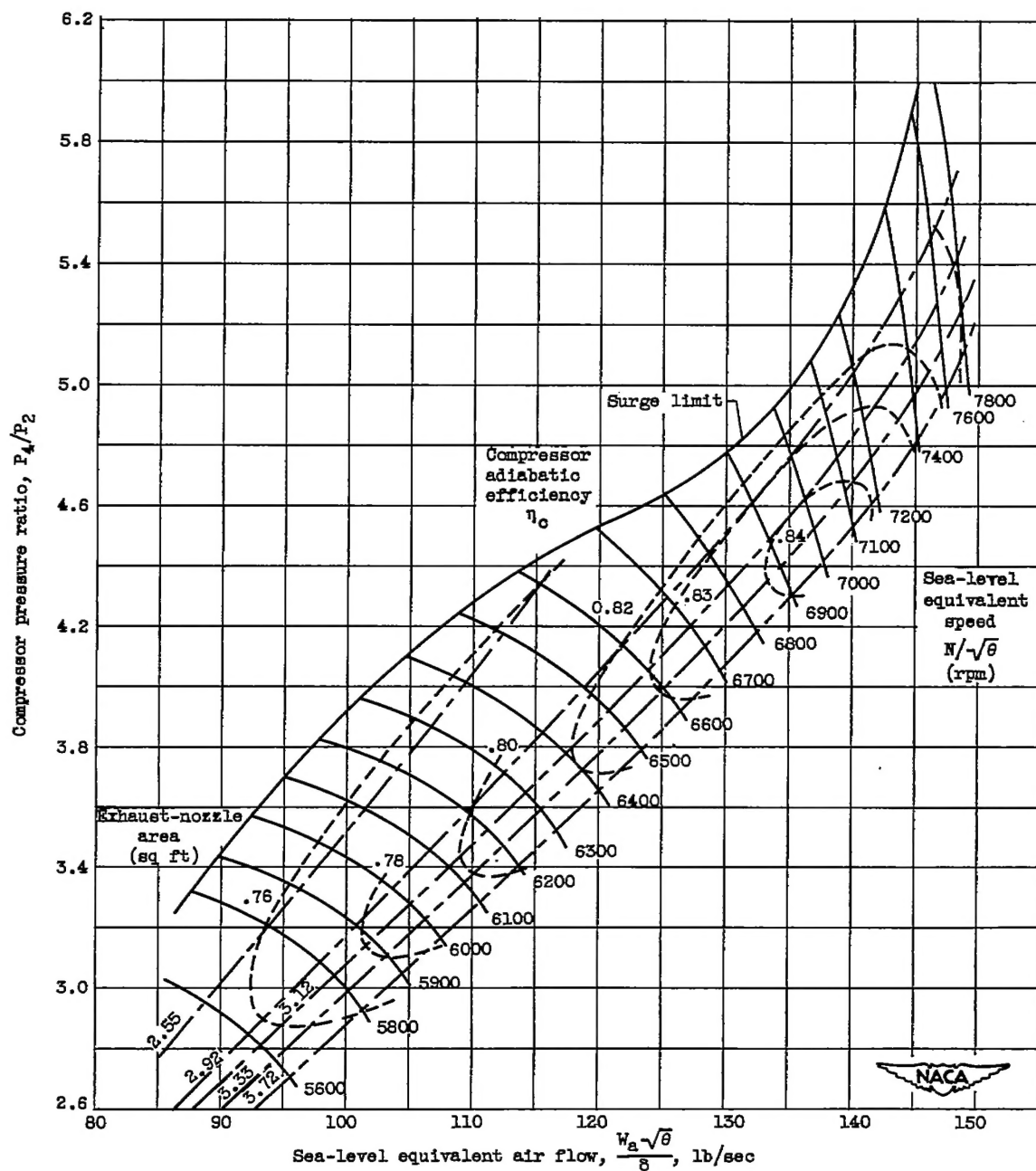Figure 13. - Surge limits and military-rated operating lines of configuration M and redesigned configuration A.

2702
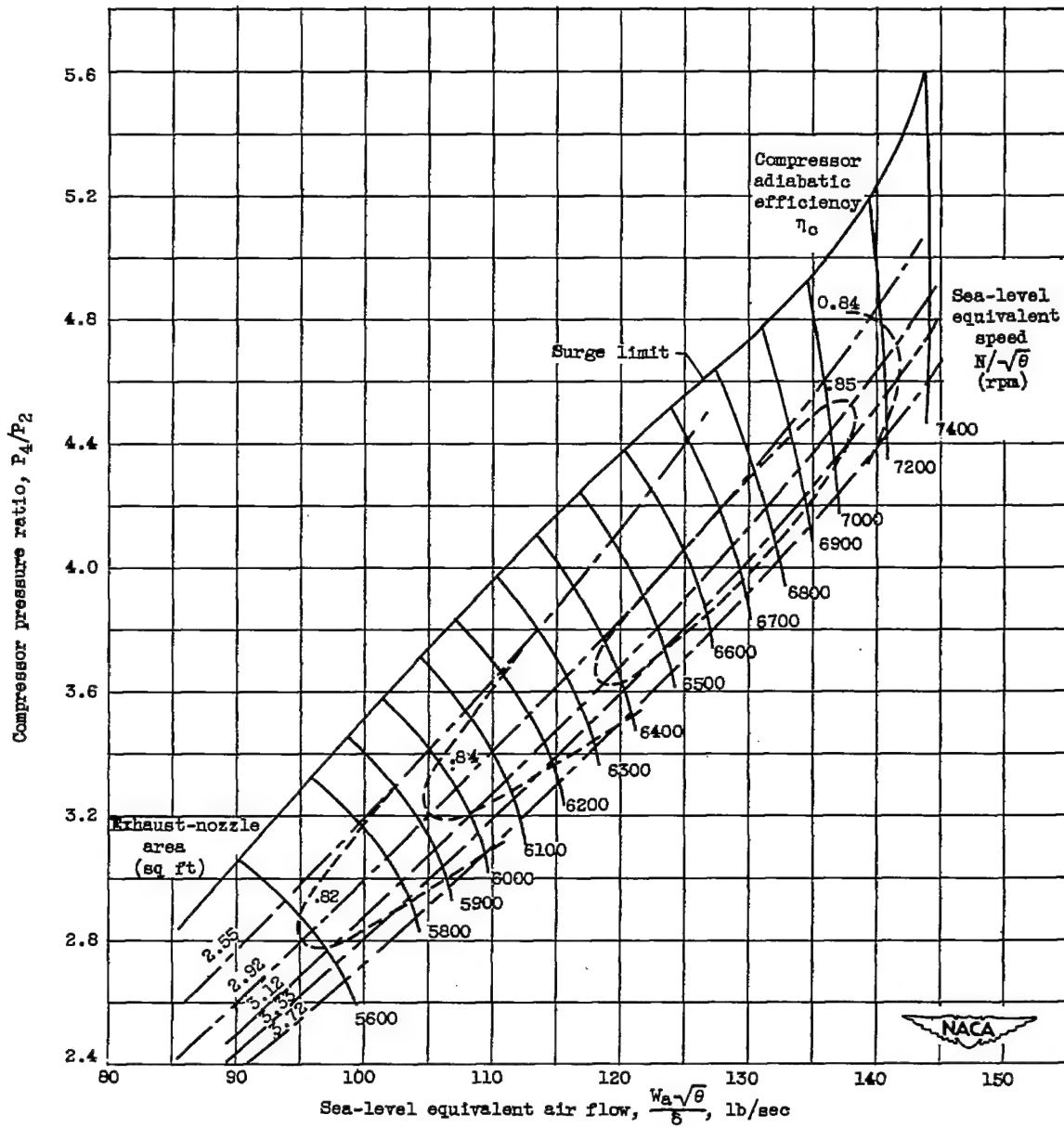
(a) Altitude, 15,000 feet; flight Mach number, 0.64.

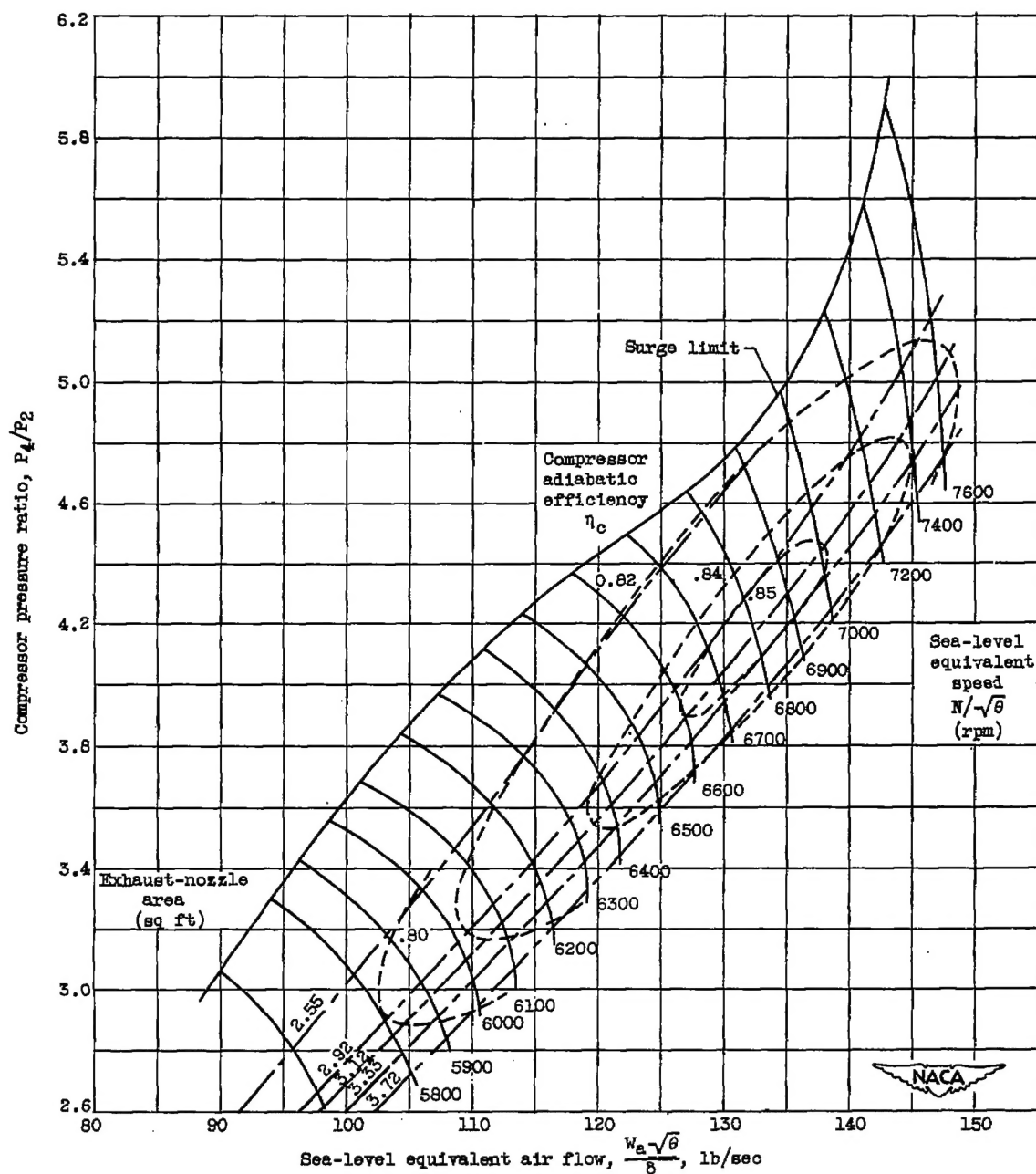Figure 14. - Compressor performance map of configuration M.

(b) Altitude, 35,000 feet; flight Mach number, 0.64.

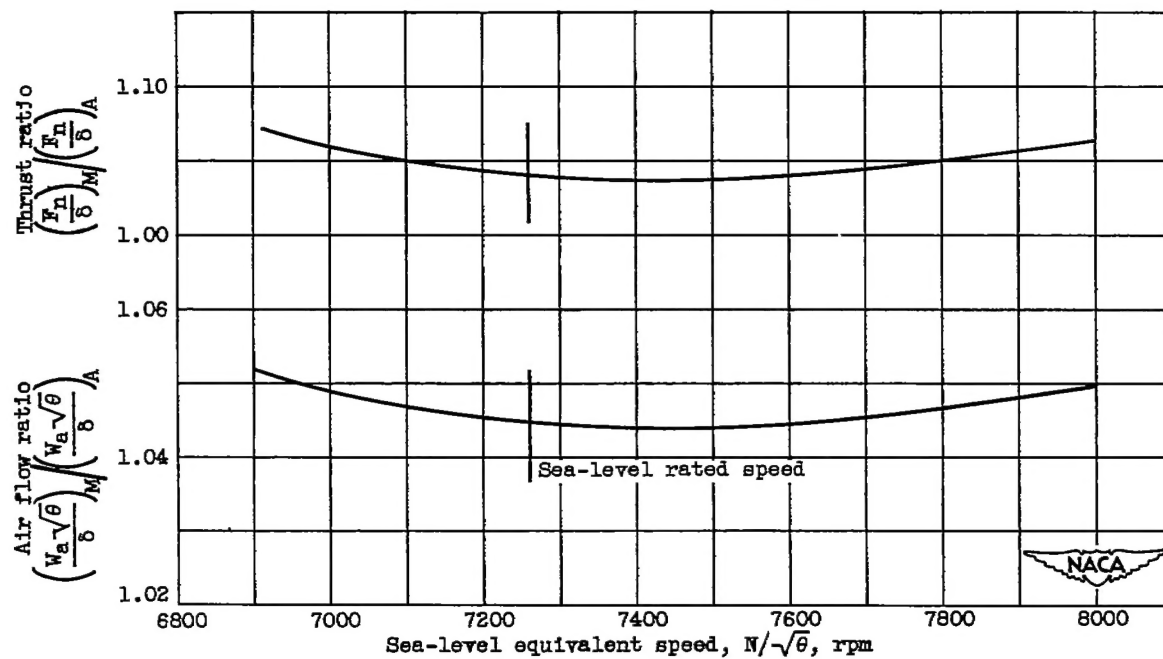Figure 14. - Continued. Compressor performance map of configuration M.

(c) Altitude, 45,000 feet; flight Mach number, 0.64.

Figure 14. - Continued. Compressor performance map of configuration M.

(d) Altitude, 35,000 feet; flight Mach number, 1.00.

Figure 14. - Concluded. Compressor performance map of configuration M.

(a) Configuration M compared with redesigned compressor (configuration A).
M, configuration M; A, configuration A.

Figure 15. - Ratios of calculated net thrust and measured equivalent air flow.
Altitude, 30,000 feet; flight Mach number, 0.64.
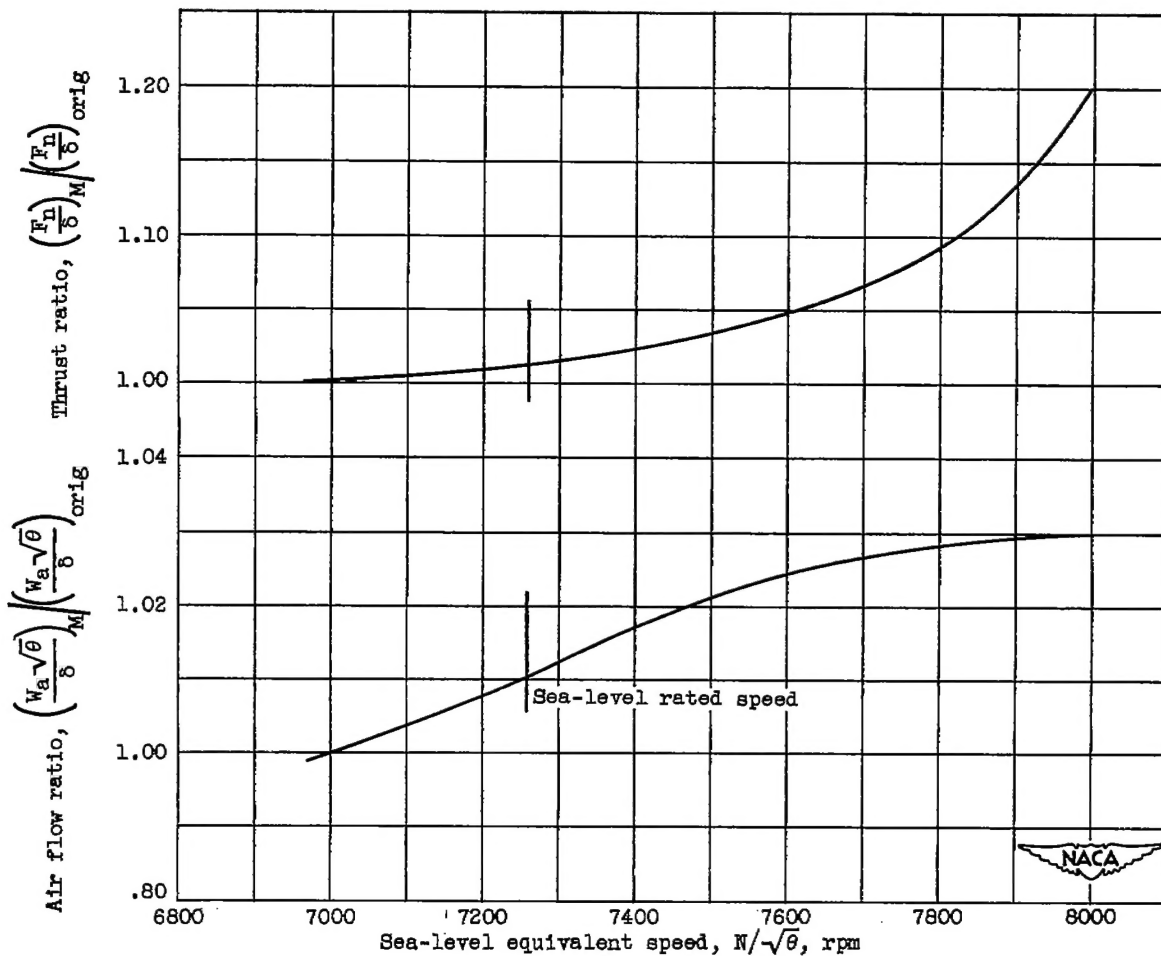
(b) Configuration M compared with original production engine (reference 1).
M, configuration M; orig, original production engine.

Figure 15. - Concluded. Ratios of calculated net thrust and measured equivalent air
flow. Altitude, 30,000 feet; flight Mach number, 0.64.